LAWRENCE
LIVERMORE
NATIONAL
LABORATORY

LLNL-TR-607653

The Hydrogen Corrosion of Uranium: Identification of Underlying Causes and Proposed Mitigation Strategies

A. Loui

December 11, 2012

Disclaimer

This work performed under the auspices of the U.S. Department of Energy by Lawrence Livermore National Laboratory under Contract DE-AC52-07NA27344.

1.1 Introduction

The corrosion of uranium by hydrogen, like the more familiar form of oxidative corrosion (e.g., rusting), is a destructive process driven by a chemical reaction. For hydride corrosion, the principal reaction is the formation of a metal hydride precipitate which has a lower mass density than that of the parent metal. The volumetric expansion of the forming precipitate within the metal can be elastically accommodated if the second-phase particles are sufficiently small (e.g., less than a micron);[1] for larger precipitates, the stresses imposed on the surrounding metal are relieved by the mechanisms of plastic deformation and/or fracture. The gross, macroscopic effects of hydride precipitation are the progressive loss of integrities both mechanical (ductility) and structural (fracture, crack propagation, component failure). Uranium hydride corrosion, as described in the open and gray literatures, falls into the latter category and specifically refers to the superficial pulverization of uranium caused by the formation and growth of uranium hydride (UH_3) precipitates near the metal surface. Since the superficial corrosion reaction is sustained by a supply of hydrogen reactant from the environment, the hydrogen corrosion of uranium is regarded in the metallurgical literature as a form of environmental hydrogen embrittlement.[2]

Simply put, any strategy conceived and developed to mitigate or prevent hydride corrosion in a uranium component must ultimately seek to minimize or eliminate the interaction of hydrogen with uranium. This essential mandate must be applied to the entire life cycle of the component, where hydrogen contamination might be introduced during the following phases: 1) early stages of the metal processing, such as annealing or pre-heating in molten inorganic salts;[3] 2) subsequent machining using cutting fluids, coolants, lubricants, and degreasing agents which may potentially form hydrogen upon reaction with uranium, particularly those that are water-based, and; 3) service life, from hydrogen-generating environmental sources. It is typically during the first phase (processing) that most of the hydrogen contamination occurs;[3] unless the uranium is rapidly quenched (e.g., 380 K/s)[4] and a supersaturated condition results, the quantity of dissolved hydrogen will exceed the solid solubility limit during cooling to ambient temperature, and hydride precipitation will occur. The result is a pre-corrosion state where UH_3 precipitates distributed throughout the component may grow into fully developed corrosion sites upon subsequent hydrogen exposure.

During the second and third life cycle phases, the metal can be protected from corrosion by isolating it from hydrogen and hydrogen-forming chemicals; such strategies are external to, and hence independent of, the component itself. If these isolation or sequestration strategies fail, the component – in a vulnerable pre-corrosion state – will be exposed to hydrogen and corrosion will ensue. Ideally then, it would be desirable to reduce the corrosion potential of the component *per se*, either by removing pre-existing UH_3 precipitates (e.g., redissolution and outgassing *via* vacuum annealing) and/or modifying the properties of the metal in such a way as to reduce its reactivity with hydrogen. In this technical report, a consensus description of hydride precipitation and subsequent growth is carefully developed from the literature on uranium hydride corrosion.

The hydride corrosion of uranium has been universally observed to be localized, spatially heterogeneous, and seemingly random (Fig. 1). This observation – that there are some locations in the metal which are apparently conducive to hydride corrosion, and others which are not (and, hence, resistant to corrosion) – is the focal point of this technical report. A listing of corrosion initiation sites most strongly supported by the literature is provided, followed by recommended strategies for treating/reconditioning uranium components to forestall the deleterious effects of hydrogen corrosion.

1.2 Initiation of Uranium Hydride Corrosion: A 'Consensus' View

Since the late 1940s, uranium hydride corrosion research has occurred in several analytical areas: 1) chemical kinetics, examining reaction rates from onset to complete destruction of the massive metal;[5,6,7,8,9,10,11,12,13] 2) metallography, elucidating the connection between corrosion and metal microstructure;[14,15,16,17,18] 3) surface chemical analysis, identifying the oxides and chemical impurities which potentiate or retard the corrosion reaction.[19,20,21,22,23] Whether the goal is a proactive treatment at the beginning of component life, or a remediative treatment (reconditioning) administered later in the life cycle, any mitigation or prevention strategy for hydride corrosion must first identify the critical conditions which *exist at, and just prior to*, the earliest stage of reaction, and then determine ways to counteract or eliminate those causative conditions. Therefore, research efforts aimed at combating corrosion require a focus on metallography and chemical analysis, such that a coherent and self-consistent picture of corrosion *initiation* – rather than an accounting of time-dependent behavior once corrosion is established and underway – may be obtained.

Despite the breadth of the literature concerning uranium hydride corrosion, certain points of definitive agreement – and, conversely, divergent conclusion – can be culled to serve as guidelines for strategic development. From the former, a 'consensus' view of corrosion initiation is formed which collectively represents the best understanding of the destructive phenomenon currently available. A truly complete and harmonious agreement is uncommon in the scientific literature, even as a topical understanding evolves and is refined over time; thus, in practice, a 'consensus' may be interpreted as an agreement approaching unanimity. In the next section, the points of near unanimity are presented, as are observations for which there is broad support but some considerable, dissenting opinion.

Connecting these points of definitive agreement is the undisputed, singular observation presented in the introduction: uranium hydride corrosion follows a localized, spatially heterogenous, and apparently random pattern of initiation. As shown in Fig. 1, the haphazard nature of hydride corrosion occurs on spatial scales of a few millimeters or less. Since partial pressure variations of H_2 reactant across the non-occluded uranium surfaces on this scale are implausible, the observed pattern of corrosion must reflect some localized property (or set of properties) of the metal itself.

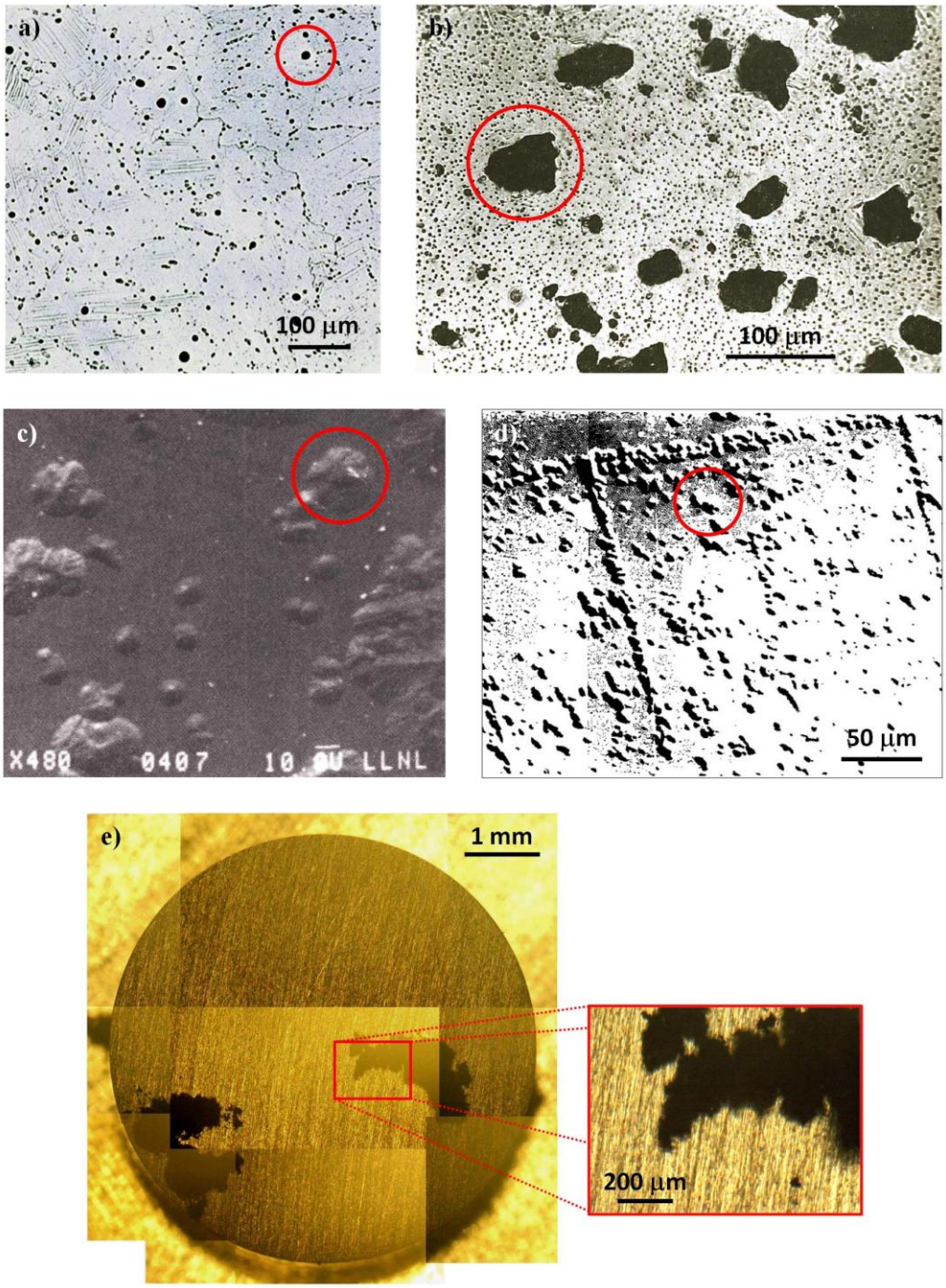

Figure 1. Observations of uranium hydride corrosion (open circles) by sites within the U.S. complex and by foreign agencies (current institutional designations listed), using optical and scanning electron microscopies (OM and SEM, respectively). a) OM image (Hanford Site, 1957).[24] b) OM image (Atomic Weapons Establishment, 1966).[25] c) SEM image (Lawrence Livermore National Laboratory, 1984).[26] d) SEM image (Nuclear Research Center – Negev, 1996).[27] e) Composite OM image (Lawrence Livermore National Laboratory, 2011).[28]

These experimental image data are not surprising when one considers the solid solubility limit of hydrogen in uranium. Experimental solubility data for α-uranium for the temperature range 667-940 K, along with a modeled extrapolation to lower temperatures, has been previously reported by Powell at the Y-12 National Security Complex.[29] Consulting this data, one finds for example that the hydrogen solubility limit in α-uranium at room temperature (293 K/20°C/68°F) is 5.1×10^{17} atoms per cm^3 of metal for a hydrogen pressure of 1 atm; this limit can be equivalently expressed as 10.5 atomic parts-per-million (appm) or 0.04 weight parts-per-million (wppm) using the mass density of α-uranium (ρ_U = 19.05 g/cm^3) and the molar masses of α-uranium (M_U = 238.03 g/mol) and atomic hydrogen (M_H = 1.008 g/mol).[30] Since the hydrogen solubility in uranium follows Sieverts law, the solubility limit is proportional to the square root of pressure;[29] hence, for example, the solubility limit at room temperature and a pressure of 0.1 atm is 0.04/√10 = 0.01 wppm. However, the concentration of dissolved hydrogen required to form stoichiometric UH_3 *throughout* the metal bulk is considerably higher; this critical concentration can be readily calculated using the expression

$$\frac{\#\ of\ H\ atoms}{cm^3\ U} = \left(\frac{3\ H\ atoms}{1\ U\ atom}\right)\left(\frac{N_A\ U\ atoms}{mol\ U}\right)\left(\frac{mol\ U}{g\ U}\right)\left(\frac{g\ U}{cm^3\ U}\right) = \frac{3N_A\rho_U}{M_U} \qquad (1)$$

where N_A is Avogadro's number. Substituting the uranium density and molar mass values, the threshold hydrogen concentration for *bulk* hydride formation is 1.4×10^{23} atoms/cm^3 or 12.7 weight parts-per-*thousand*. From these calculations, it is evident that the scant quantity of environmental hydrogen which can dissolve into uranium at modest partial pressures and temperatures is six orders of magnitude too small to achieve *homogeneous* hydride formation. Therefore, any UH_3 formation must occur locally rather than globally, where the small number of dissolved hydrogen atoms can aggregate and exceed the critical concentration at isolated locations.

While this simplistic explanation is wholly supported by the universal observations of localized and heterogeneous hydride corrosion, an essential question is raised: what is special about the metal at the sparse locations where hydride corrosion is observed to occur, that allows hydrogen to locally accumulate in sufficient concentration to form UH_3, compared to the remaining bulk? Any practical metal component does not exhibit a perfect crystalline microstructure throughout its bulk, but is filled with randomly occurring defects. This random quality would be obviously reflected in the spatial distribution of corrosion sites, if a simple and direct correlation with defects existed. Variations in apparent corrosion initiation potential amongst defects could be explained plausibly by the wide variety of defect types which exist: misorientation boundaries (grain and twin boundaries), dislocations, voids, impurities, and second-phase particles. Such a facile association of hydride corrosion initiation with defects seems natural and almost self-evident; however, is this glib conjecture supported by the literature?

1.3 Experimental Evidence for UH_3 Corrosion Initiation Sites

1.3.1 Relationship of Corrosion to Defects

A thorough review of uranium hydride corrosion reports, spanning seven decades and primarily focused on metallography and chemical analysis, reveals overwhelming evidence that at least some types of defects are correlated with corrosion initiation. A localized mode of nascent corrosion was observed in early uranium hydride studies by optical microscopy.[24,31] Albrecht and Mallett, in their 1956 kinetics study, reported the rapid formation of an apparently uniform hydride film; however, this observation was made visually without the benefit of optical magnification.[6]

With virtually no reports to the contrary, a strong correlation of hydride corrosion to *misorientation boundaries* on uranium has been repeatedly observed. Adamson and co-workers at the Atomic Weapons Establishment (AWE, using the current institutional designation) reported no obvious link between hydride precipitation and grain boundaries in their fractographic experiments using optical and transmission electron microscopies (OM and TEM, respectively);[32] however, other contemporary research found compelling evidence to the contrary.[4,33] More recently, Moreno, Arkush, and co-workers at the Nuclear Research Center, Negev (NRC-Negev) observed aggressive hydride corrosion – and presumed prior nucleation – at twin and grain boundaries using scanning electron microscopy (SEM).[15,34] In a study of hydrogen and water vapor adsorption and reaction on uranium at Lawrence Livermore National Laboratory (LLNL), Balooch and Hamza directly observed the growth of uranium hydride at grain boundaries using atomic force microscopy (AFM).[16] Bingert and co-workers at Los Alamos National Laboratory (LANL) used SEM and electron backscatter diffraction (EBSD) to investigate the uranium-hydrogen reaction;[17] they found that 78 of 101 identified hydride sites could be correlated to a high- or low-angle grain boundary, or to a twin boundary. SEM images obtained at LLNL and LANL by Siekhaus and Schulze (respectively) after the uranium-hydrogen reaction is allowed to progress to the pitting stage also show a strong correlation to grain boundaries.[18] Scott and co-workers at AWE observed uranium deuteride sites exclusively at uranium grain boundaries in secondary electron images;[23] the chemical identity of these sites was confirmed in spatial maps of several deuterium-containing positive ions. As is frequently done in secondary ion mass spectrometry (SIMS) studies, deuterium was substituted for hydrogen to allow differentiation of the corrosion reactant from background sources of hydrogen (e.g. residual water) and to simplify interpretation of ion mass fragments. Such observations on uranium deuteride should be representative of uranium hydride behavior, as differences in reactivity between hydrogen isotopes and uranium have not been observed.[35] Some of these published results are shown in Fig. 2.

There is also broad support for corrosion initiation at *inclusions* on uranium, particularly monocarbides exhibiting the characteristic cubic NaCl crystal geometry, although there are comparatively more dissenting opinions for this type of defect. Using OM, Owen and Scudamore

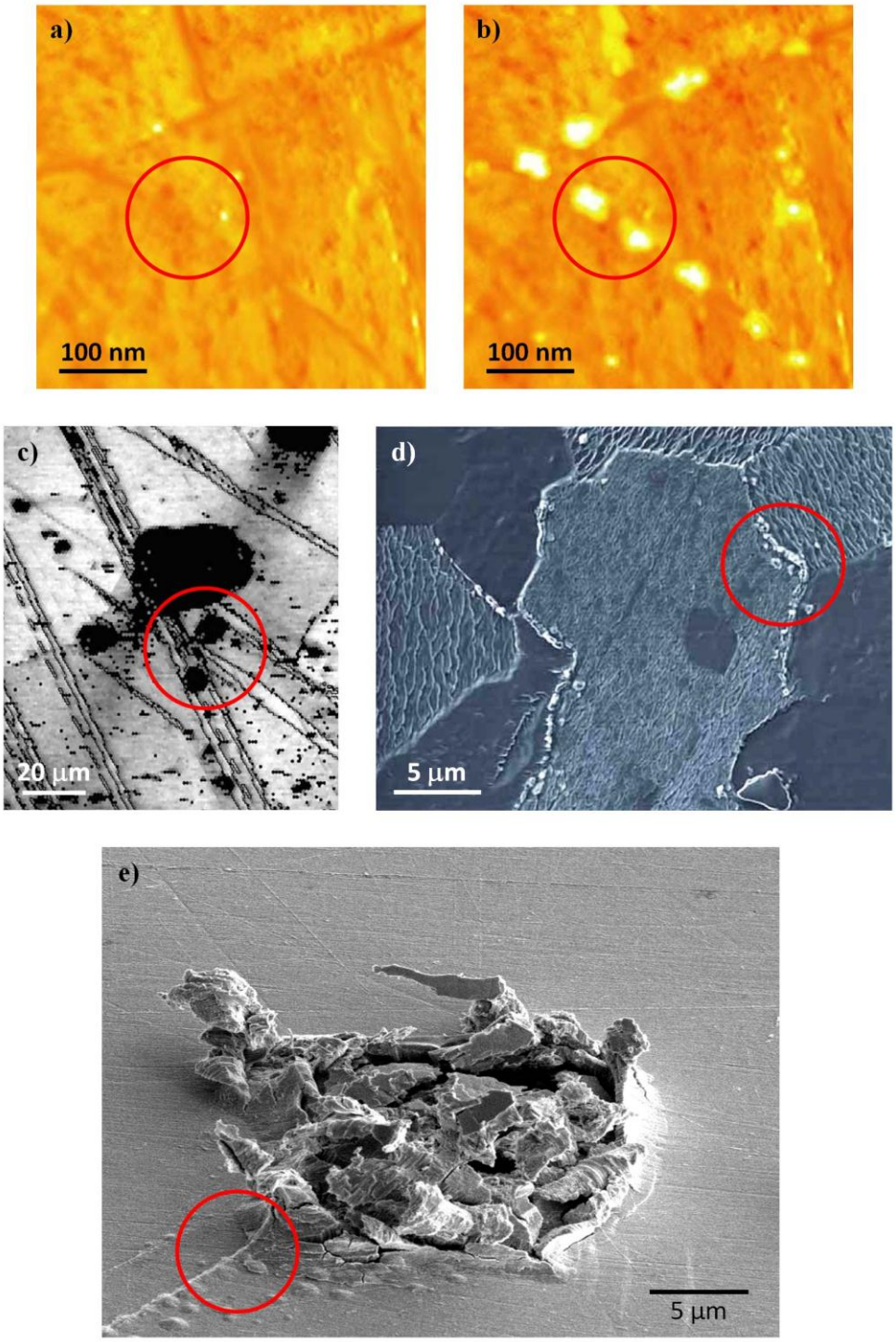

Figure 2. Observations of uranium hydride corrosion at misorientation boundaries (open circles) by sites within the U.S. complex and by foreign agencies (current institutional designations listed). a) and b) AFM image sequence (LLNL, 1996).[16] c) EBSD image quality map (LANL, 2004).[17] d) SIMS secondary electron image (AWE, 2007).[23] e) SEM image (LLNL, 2009).[18]

(AWE) observed that the most aggressive hydride corrosion occurred at inclusions, although they also reported the occurrence of a finer dispersion of slowly-reacting hydride spots.[25] In addition to preferential corrosion at misorientation boundaries, Moreno, Arkush, and co-workers (NRC-Negev) also documented a correlation between hydride formation and inclusions.[15,27] A similar conclusion was reached by Siekhaus (LLNL) and Schulze (LANL), based on their respective SEM data of uranium hydride pitting corrosion.[18] While Bingert and co-workers (LANL) found an apparent association of small carbide inclusions (less than ~20 μm) with deformation twins – the same type of misorientation boundary identified as likely corrosion initiation sites – they concluded that no definitive correlation existed between larger carbide inclusions and uranium hydride formation.[17] The secondary ion mass spectrometry (SIMS) study of Scott and co-workers (AWE), in which an exclusive association of deuteride corrosion sites with grain boundaries was revealed, found no spatial coincidence of deuterium-containing and carbon-containing positive ion maps on uranium.[23] Although these authors concluded that deuteride corrosion was not correlated with carbide inclusions, a contemporary SIMS study performed at LLNL found that negative (versus positive) deuterium-containing ion maps were of higher relative intensity and appeared to provide the highest fidelity chemical mapping of the corrosion product on uranium.[22] If this were also true of carbon-containing negative ion maps, it is possible that the AWE study simply failed to spatially resolve deuteride corrosion sites associated with carbide inclusions.

1.3.2 Interpretation of Experimental Evidence: Correlation vs. Causation

The preponderance of experimental evidence supports the correlation of uranium hydride corrosion to defect sites, although it is clear that there are dissenting opinions on which types potentiate the phenomenon. A more fundamental, and controversial, issue is the progression from *correlation* to *essential causation* – does the observation of hydride corrosion at uranium defect sites necessarily imply that the sites themselves are the root cause of corrosion? Or is the association more coincidental in nature? Certainly, an elucidation of this causal relationship would be abetted by the direct observation of corrosion initiation, as it is actively occurring; less ideal would be observations made in the moments just prior to, and immediately following, the initiation event – to wit, a 'before and after' comparison. In most of the published studies on uranium hydride, observations of the corrosion product some time after the initiation event (i.e., post-mortem) are reported. This is typically the result of instrumental limits in spatial resolution, preventing observation of corrosion spots in the nascent stages of growth when they are smallest. Another common case is the inability to perform controlled hydridation experiments *in situ* within the experimental apparatus, imposing a transfer delay between reaction and imaging facilities. Nevertheless, despite the near absence of the most compelling form of evidence (i.e., corrosion 'caught in the act'), researchers have had no difficulty in interpreting post-mortem data on hydride corrosion sites as implying prior initiation at the same locations.

Despite the near unanimity in associating hydride corrosion with at least certain types of defects, there is a considerable divergence of opinion on causation. Researchers at AWE and NRC-Negev

regard the metal-borne defects to be of secondary importance to corrosion initiation, and instead identify the properties of the superficial oxide layer – namely, thickness and mechanical integrity – as the determinants of initiation site.[36,37] In this point-of-view, the localized and spatially heterogenous pattern of uranium hydride formation reflects a corresponding pattern of environmental hydrogen penetration through the imperfectly protective oxide to the underlying uranium. The original model of Glascott (AWE) is based on purely diffusive hydrogen penetration of a defect-free oxide layer (i.e., oxide lattice diffusion) to the metal, and an ensuing corrosion reaction at the oxide-metal interface;[38] similar Fickian transport models, describing subsequent hydrogen penetration into and reaction with the uranium bulk, were previously presented by Condon and Kirkpatrick (Y-12) and are regarded as the definitive theory on the hydride corrosion kinetics of massive uranium.[9,10,13] In this version of the Glascott model, the spatial heterogeneity of corrosion initiation is entirely due to a random distribution of oxide thicknesses, with initiation occurring first where the oxide barrier is thinnest. Such a distribution of thicknesses would be expected if oxide growth rate varied with the crystallographic orientation of different uranium grains, which Moreno and co-workers (NRC-Negev) claim will occur if the oxide grows epitaxially and hence with orientations aligned with the underlying metal grains.[15] Prior X-ray diffraction (XRD) measurements by Orman and co-workers (AWE) found no such epitaxial oxide growth at 200°C and a pressure of 4 Torr for layer thicknesses crudely estimated at less than 1 μm, but the appearance of some preferential orientation for comparatively thicker layers formed at higher oxygen pressures.[39] These data are consistent with a modest variation in oxide diffusivity with crystallographic orientation, which becomes significant only under conditions of increased adsorbed concentration (scaling with pressure) and elevated temperature. Without further information, it can be speculated that epitaxial growth at the significantly lower temperatures where most practical uranium oxides are formed (e.g., room temperature) may still occur if the oxygen pressure is sufficiently high (e.g. 159 Torr in ambient air) to offset the lower diffusivity. In such a case, an overall diffusive flux, with a sufficient magnitude to exhibit anisotropy with underlying grain orientation, may be obtained.

Aside from establishing a plausible mechanism for the existence of a random distribution of oxide layer thicknesses, there is a more fundamental difficulty concerning a uranium corrosion initiation model based on oxide lattice diffusion. Siekhaus observed that the experimentally measured solubility of hydrogen at room temperature and a partial pressure of 1 atm is 5×10^{17} cm^{-3} in uranium (as described above in Section 1.2), while only a meager 7×10^{3} cm^{-3} (extrapolated from the data of Sherman and Olander)[40] in uranium dioxide;[41] therefore, the spontaneous diffusion of dissolved hydrogen from the oxide to the metal is highly thermodynamically unfavorable. More recent versions of the Glascott model have partially addressed this issue by incorporating boundaries at the interfaces of both fine and coarse oxide grains as additional pathways for environmental hydrogen penetration to the uranium metal;[42] however, the random distribution of oxide thicknesses is retained, as is premise of oxide lattice diffusion. Bazley and co-workers (AWE) described a circumstantial validation of the model in a recent report on uranium hydriding kinetics at various reaction temperatures.[43] They found that

inverse corrosion initiation time appeared to follow a simple power law in hydrogen pressure. Arrhenius plots of the proportionality factor – an effective reaction rate constant incorporating the physical assumptions of the Glascott model – with respect to inverse temperature yielded an activation energy value (57 kJ/mol) close to a value previously reported by Wheeler (AWE) for hydrogen lattice diffusion through single-crystal uranium dioxide (60 kJ/mol).[44] In their SIMS study, Scott and co-workers conjectured on the compatibility of their observations of grain boundary corrosion attack with the current Glascott model:[23] should oxide grow epitaxially on uranium grains, mismatched oxide grain boundaries – a pathway for environmental hydrogen penetration – would occur above uranium grain boundaries, making these favored sites for corrosion initiation. They also note, in implicit accordance with the model, that the deuteride corrosion growths appeared to initiate at, or within 0.5 μm below, the oxide-metal interface. These endorsements, which illustrate the solidarity of the AWE stance, emphasize their belief in the preeminent role that an imperfectly protective oxide layer plays in determining the spatially heterogeneous pattern of localized hydride corrosion initiation.

In comparison, researchers at NRC-Negev assign a much more causative role to misorientation boundaries, inclusions, and other types of defects in the underlying uranium metal, which they typically refer to as "*physical discontinuities.*"[15,27] Moreno and co-workers stated that such defects "*cause a misfit in the continuity of the oxide layer or a physical gap in it*" such that environmental hydrogen diffuses more rapidly "*through the misfit interface area formed between the grown oxide layers which are correlated with the microstructure.*"[15] Ben-Eliyahu and co-workers further implicated these defects as defining locations where small hydrides may grow beyond a limited size (due to compressive constraint from the overlying oxide) and mature into fully developed corrosion sites;[37] these authors dub the former locations "nucleation sites" and the latter "growth centers" to emphasize the difference in corrosion initiation potential. Using SEM, Arkush and co-workers observed the appearance of surface features of ~1 μm diameter and a number density of 10^3-10^4/mm^2 following a 60 second hydrogen exposure (750 Torr) at 50-75°C, which they identified as the compression-limited nucleation sites;[27] Harker and Chohollo (AWE) reported similar features with a density of ~2×10^3/mm^2 following a 45 second hydrogen exposure (7.5 Torr) at ~80°C.[45] In the recent hydriding kinetics study of Bazley and co-workers, OM observations with a minimum resolution threshold of ~30 μm revealed a considerably lower density of corrosion sites (~0.01/mm^2) following a ~60 second hydrogen exposure (750 Torr) at 75°C;[43] given their size and increasing diameter,[46] these hydride sites are consistent with the "growth centers" defined by Ben-Eliyahu and co-workers.

In the foregoing discussion, it should have been evident that there are some assumptions of uncertain veracity – most prominently, the occurrence of epitaxial oxide growth on uranium grains, leading to a spatial distribution of oxide layer thicknesses as well as oxide grain boundaries. However, it should also have been clear that there is otherwise little controversy regarding the characteristics of the uranium hydride corrosion process, that: 1) environmental hydrogen must penetrate through an imperfectly protective oxide to reach the metal, with which it ultimately reacts to form the corrosion product; 2) the corrosion is closely correlated with

crystalline defects in the metal – including misorientation boundaries and inclusions and; 3) that these metal defects abet the corrosion process by creating associated pathways through the overlying oxide through which environmental hydrogen can penetrate.

What continues to be a point of dissension in the community of uranium hydride research at large is the issue of 'essential' causation, with AWE and NRC-Negev putting the primary focus and 'blame' on the oxide layer (and imperfections thereof) rather than the underlying metal (and imperfections thereof), while other institutions such as LANL hold the opposite opinion, relegating the oxide layer to a secondary role while implicating the metal properties.[17] The chief goal of the present report is to define strategies for mitigating or preventing uranium hydriding corrosion; therefore, it is crucial that the root causes be identified – whether they lie with the oxide or the metal – such that specific remedies can be conceived and developed.

To help clarify the issue, consider the following scenario and question: if the oxide layer is entirely removed from a uranium sample, and subsequently exposed to environmental hydrogen, where upon the metal surface should corrosion occur? The imperfectly protective oxide is portrayed by AWE and NRC-Negev as a sort of 'leaky' stencil or patterning mask on the metal; when the incident flux of hydrogen encounters this barrier, the reactant initially passes through only at the random scattering of locations where it is particularly thin or marked by a discontinuity (e.g., a grain boundary). If oxide lattice diffusion is permitted, as in the Glascott model of AWE, hydrogen would eventually diffuse through even the thickest layers (hence, 'leaky'). The resulting random pattern of hydride corrosion initiation – which, as noted in Section 1.2, has been universally observed – is taken to be evidence of this 'stencil'-type of mechanism. In such an 'oxide-centric' model, it is assumed that corrosion will occur at any location where environmental hydrogen successfully reaches the metal. If all these provisions are accepted, then a complete removal of the oxide should expose the entire uranium surface to hydrogen flux all at once, and corrosion should occur at all locations indiscriminately. As shown in Section 1.2, the bulk uptake of hydrogen by uranium at moderate temperatures is approximately six orders of magnitude less than that required for the formation of stoichiometric UH_3. Substantial relative enhancements in adsorbed surface concentration can be ruled out; the hydrogen sticking coefficient on uranium was measured by Balooch and Hamza (LLNL) using temperature programmed desorption, revealing an apparent saturation coverage of 0.15 hydrogen atoms per uranium atom, far below the critical threshold for hydride formation.[16] This work represents the closest realization of the proposed scenario, as it combined several experimental features not simultaneously implemented in the other studies cited above: 1) the total removal of superficial oxide *in situ* within the corrosion reaction chamber, *via* successive cycles of argon ion sputtering just prior to hydrogen exposure; 2) non-oxidizing conditions of ultrahigh vacuum (2-6×10^{-10} Torr) for the duration of the measurements; 3) nanometer spatial resolution in both surface parallel and normal directions using AFM and; 4) direct observation of the corrosion reaction as it was actively occurring, beginning with initiation (i.e., corrosion 'caught in the act'). As can be clearly observed in Fig. 2a and 2b, hydride corrosion initiated at the grain boundaries of a denuded uranium surface despite a uniform flux of hydrogen reactant to all parts of the

exposed metal. This highly heterogeneous pattern of reaction, resulting even in the absence of an intervening oxide layer, seems to definitively indicate that the 'essential' causation lies in the localized properties of the metal and not with the overlying oxide.

It must be stressed that this conclusion does not discredit the key properties of the hydride corrosion process which have been put forth and advocated by AWE and NRC-Negev; rather, the disagreement represents a divergence of deductive reasoning in arguing root causation from the collective evidence at hand. In the case of NRC-Negev, the oxide is assigned the central moderating role in hydride corrosion through its inhibitory effect on developing nucleation sites;[37] yet, even when they described how defects endow neighboring nucleation sites with the ability to develop into full-blown corrosion sites (i.e., "growth centers"), they chose to focus on the associated oxide breach rather than the metal defect which gave rise to the breach. Clearly, within the model construct that they themselves have defined, fully developed hydride corrosion at "growth centers" would not occur in the absence of metal defects. The supposition described by Scott and co-workers – that epitaxial oxide growth on uranium grains would lead to a coincidence of oxide and uranium grain boundaries[23] – is taken as validation of the Glascott model, which is wholly based on hydride corrosion initiation at oxide breaches (e.g., oxide grain boundary) or other locations of diffusive vulnerability (e.g., thin spots).[38] However, while observing grain boundary corrosion attack, these authors also chose to focus on the associated oxide breach rather than the metal defect (i.e., the uranium grain boundary) which supposedly created it. A critical difference in the AWE case is that, with the inclusion of oxide lattice diffusion in the model, fully developed hydride corrosion is presumed to occur even in the absence of such a defect, as the only impediment to reaction that is implied is the oxide barrier itself. The arguments above, based on hydrogen solubility, seem to preclude this possibility: it is not enough that reactant merely penetrate the oxide layer in a spatially heterogeneous pattern of vulnerable spots, but that a special condition of the metal at those locations must also exist for corrosion to ensue – namely, the availability of defects that the researchers at NRC-Negev invoke in defining "growth centers."

Perhaps this final phrasing of the problem best illustrates the origin of the divergent views on uranium hydride corrosion: a focus on the oxide layer as a hydrogen diffusion barrier demands an emphasis on *temporal* behavior (kinetics), while a focus on local properties of the metal that engender corrosion initiation demands an emphasis on *spatial* behavior. As the most eminent example, there is extensive documentation on the role of oxide stoichiometry, thickness, and the presence of adsorbed impurities on the reaction onset delay from initial hydrogen exposure (i.e., *induction time*) and the *rate* of corrosion site nucleation.[8,10,47,48,49,50] The various reports from researchers at Y-12, LANL, AWE, and NRC-Negev agree on the basic mechanism underlying these relationships: interstitially dissolved oxygen in superstoichiometric oxide, along with other impurity species, hinder the diffusion of atomic hydrogen; meanwhile adsorbed impurities, such as H_2O, effectively outcompete environmental hydrogen for surface sites at which dissociative chemisorption to atomic hydrogen would occur. These mechanisms determine the rate at which environmental hydrogen will reach the uranium metal, and provide the best current

understanding of the temporal aspects of uranium hydride corrosion; however, they have no intrinsic relation to the spatial aspects of the reaction, and thus can hardly be employed to explain the spatially heterogeneous reactivity of uranium towards hydrogen.

1.4 Theoretical Evidence for UH_3 Corrosion Initiation Sites

As presented in Section 1.3.1, a preponderance of experimental evidence supports the correlation of defect sites to uranium hydride corrosion initiation, with some divergent opinions on which types (e.g., inclusions) potentiate the phenomenon. The foregoing discussion (Section 1.3.2) presented an argument that the 'essential' causative factor for corrosion initiation is associated with properties of the metal rather than the overlying oxide: namely, defects. Some recent theoretical studies have provided physical insight into why such metal defects possess a high corrosion initiation potential when compared to the metal bulk. To investigate uranium hydride corrosion initiation, Taylor and Lillard (LANL) modeled the interaction of atomic hydrogen (H) with a uranium surface using density functional theory (DFT).[51] In accordance with the best practices for *ab initio* modeling of material surfaces, these authors effectively created a semi-infinite α-uranium (001) surface using a 96-atom, three-layer substrate slab terminating in a vacuum gap and subjected to three-dimensional periodic boundary conditions. The resulting supercell, incorporating H at various high symmetry sites, was energetically and structurally optimized via iterative minimization algorithms. These calculations show that penetration of H through a defect-free metal surface is energetically unfavorable and in excess (by a factor of 2) of experimentally measured activation barriers for H uptake by uranium.

By varying the hydrostatic lattice strain from compressive to tensile, Taylor and Lillard also found a significant decrease in H binding energy upon application of tensile stress to the metal with, for example, a predicted value of approximately 0.28 eV (6.5 kcal/mol) at +0.5% volumetric strain at square pyramidal sites.[51] In comparison, an Arrhenius fit to the experimental solubility data of Powell for hydrogen in uranium[29] gives an estimated activation barrier of 0.29 eV,[41] while several other experimental studies report values in the range 0.26-0.35 eV.[9,11,52] This strain amplitude is within the elastic regime; a uniaxial static tensile strain of about 1% was measured by Garlea and co-workers (Y-12) for cast depleted uranium at its tensile yield strength of ~275 MPa,[2] giving an estimated hydrostatic strain value and elastic limit of 3%.

Furthermore, the LANL DFT calculations for *bulk* octahedral sites adjacent to a substitutional atomic impurity (C, Ne, S, and Si) show that H binding energies can be significantly reduced (C: -30%; Ne: -47%; S: -70%) or completely eliminated (Si: -117%).[51] In contrast, quantum chemistry calculations by Balasubramanian (LLNL) on idealized (i.e., non-optimized geometry) uranium clusters with a substitutional *surface* impurity show enhanced dissociation barriers for molecular hydrogen at a C impurity (+82%) and reduced barriers at a Si impurity (-45%).[53] Aside from the fundamental differences in computational approach, the LLNL and LANL results for C are not necessarily contradictory as they technically address different phenomena: molecular hydrogen may not favorably dissociate into atomic hydrogen at a surface carbon site,

and atomic hydrogen, once created by whatever mechanism, may energetically favor binding at a carbon site within the bulk. The above conclusions concerning silicon find support in isovolumetric kinetics experiments reported by DeMint and Leckey (Y-12) on uranium hydriding rates, which showed a 50% reduction in the hydriding time of α-uranium with Si content exceeding about 100 wppm.[54] When these authors fitted their data to the hydriding kinetics model of Condon and Kirkpatrick (Y-12),[9,10,13] they found that uranium spallation resulting from the corrosion reaction was predicted to increase with increasing Si content. Since the uranium reacts directly with hydrogen in its dissolved monatomic state, spontaneous H absorption near bulk Si impurities (as predicted by the LANL calculations) is consistent with the observed enhancement in reaction rate, as is an increase in H availability near surface Si impurities (as predicted by the LLNL calculations). Interestingly, the LANL study concluded that the similar reduction in H binding energy induced by a chemically inert Ne atom, when compared with the other impurity species examined, showed that bonding considerations were not a factor, but rather indirect strain effects on the local geometric and electronic structure. Due to the static structural nature of the LLNL quantum chemistry calculations, a similar conclusion on strain effects cannot be drawn. Balasubramanian also performed similar calculations on the interaction of a uranium atom in the +3 oxidation state with molecular hydrogen, and found that a complex was formed spontaneously which leads to the dissociation of the molecule;[55] this result suggests that uranium hydride itself is a catalyst for the formation of atomic hydrogen, a process regarded as the earliest critical step in the corrosion process.

These theoretical results provide some insight into the hydride corrosion initiation behavior described in Section 1.3.1. Taylor and Lillard found that entry of adsorbed atomic hydrogen into the uranium bulk *via* lattice diffusion was energetically prohibitive; since hydride corrosion is known by direct observation to propagate into the metal bulk – see Ref. 11 for a dramatic example – the hydrogen reactant must instead make inroads at lattice defects such as misorientation boundaries, and the interfaces between inclusions (or other second-phase particles) and the parent metal. This would explain why, as seen in Fig. 2a and 2b, an oxide-free uranium surface exhibits corrosion initiation at grain boundaries instead of facets following exposure to hydrogen.[16] The strong predicted barrier to H diffusion through exposed grain facets also seems to preclude the basic assumption of oxide lattice diffusion in the Glascott model (AWE), as described in the previous section: hydrogen which successfully penetrates through a thin spot in the oxide layer will most commonly encounter a uranium grain facet; unable to develop a sufficient local surface (Section 1.3.2) or bulk (Section 1.2) concentration to form UH_3, corrosion will fail to initiate at such locations.

The LANL DFT results basically show that localized tensile stresses in the uranium lattice decrease energetic barriers to H dissolution; since such stress fields typically occur in the locality of a defect, dissolved hydrogen is expected to accumulate preferentially at those sites. In a separate study, Taylor and Lillard found that the 3:1 H/U concentration ratio necessary for the formation of UH_3 become more energetically favorable at places where the lattice can more readily expand to accommodate interstitial hydrogen – grain boundaries or interface surfaces,

vacancies, and voids.[56] These findings, derived from first principles, thus provide an elementary picture of uranium hydride corrosion: random lattice defects act as hydrogen sinks, some allowing a critical concentration of dissolved hydrogen to nucleate UH_3, which ultimately gives rise to a localized and spatially heterogeneous pattern of nascent corrosion. That this facilely derivative prediction has been universally observed (Fig. 1) lends credence to the essential correctness of the computational results.

Nevertheless, the body of experimental literature on the uranium-hydrogen system is virtually silent on the notion of defect-related strain as the causative factor for the observed association between defects and corrosion initiation. In their 2004 study, Bingert and co-workers (LANL) stated that "*observed variations in hydride nucleation rate and distribution*" for metal-borne initiation would be the result of either: 1) a dependence of hydrogen diffusivity on crystalline orientation relationships in the metal, or; 2) "*the accommodation of hydride nucleation and growth at defect regions based on considerations of reduced strain energy*."[17] The first phenomenon – a diffusivity variation with orientation – was invoked by Moreno and co-workers (NRC-Negev) as the reason for differential oxide growth rates on variously oriented uranium grains, and hence resulting misorientation boundaries in the oxide layer (Section 1.3.2); in contrast to the LANL study, this behavior was used by the researchers at NRC-Negev to argue in support of oxide-borne initiation.

On the other hand, the same body of literature is replete with studies on the chemical kinetics of the ensuing corrosion reaction, of which there are a few notable discussions on the effects of lattice strain. Strain effects on uranium hydride growth kinetics have been accounted in the landmark series of papers by Condon and Kirkpatrick.[9,10,13] Note that 'growth kinetics' denote the corrosion behavior *once the reaction is well-established*; in the case of massive uranium samples exposed to environmental hydrogen, linear reaction rates (zero-order kinetics) are observed during pitting corrosion and subsequent coalescence of pits into a reaction front which advances into the metal bulk.[9,13] It should be evident that any discussion of kinetics, by definition, involves mechanisms which operate *following* initiation and are therefore temporally distinct. The corrosion kinetics model of Condon and Kirkpatrick incorporates the large volume expansion upon hydride formation (~75%), leading to a loss of metal integrity once its ultimate strength is exceeded; therefore, the local conditions of strain determine whether gaseous hydrogen has direct access to the growing hydride exposed by the fractured metal, or must continue to diffuse through intact metal. Bloch and Mintz (NRC-Negev) speculated that expansion of the lower density hydride in the metal promotes ensuing growth at the hydride-metal interface (versus new nucleation in the bulk) as a means of minimizing strain, thus giving rise to the sharply defined corrosion reaction front that is observed in post-mortem cross sections.[11] In a subsequent study, they also theorized that hydride expansion in uranium creates a strain field in the surrounding metal that effectively hinders the development of precipitates in the bulk versus the surface when exposed to gaseous hydrogen;[14] these arguments were based superficially on comparisons to hydride growth in holmium, where precipitation of holmium hydride – which experiences only a 9% volume expansion – is observed to occur in the bulk both

inter- and transgranularly. A similar mechanism is invoked by Ben-Eliyahu and co-workers (NRC-Negev) to explain the apparent growth suppression of some nascent hydride corrosion spots ("nucleation centers") versus others ("growth centers");[37] in this case, the compressive strain field is created by the overlying oxide, where it is presumed that the burgeoning spots are located precisely at the oxide-metal interface.

The effect of metal lattice defects has also been considered in the context of uranium hydride corrosion kinetics. Condon observed that cold worked uranium experienced reduced hydriding rates compared to cast material,[9] such as that most likely used by Wicke and Otto;[7] well-annealed samples (e.g., 600°C for one day) then produced highly uniform reaction rates that closely matched the prior study. This behavior was accounted in subsequent studies by Powell and co-workers (Y-12),[12,29] and Bloch and Mintz (NRC-Negev),[57] and recognized by Harker (AWE).[36] The hallmark of cold working – whether obtained by hydroforming, rolling, or shearing – is the proliferation of dislocation and twin boundary defects, and this localized plastic deformation can be reversed by annealing the metal to sufficiently high temperatures to allow a thermally-driven recrystallization to occur (i.e. recovery). The implication of lattice defects in both uranium hydride corrosion initiation and the following growth behavior is unlikely to be coincidental, and points to a common underlying physical mechanism or set of mechanisms. The theoretical studies of Taylor and Lillard, and Balasubramanian, explored some of these defect associated mechanisms; in the next section, we consider the experimental and theoretical literature on other hydride-forming metals to gain further insight.

1.5 Corrosion Initiation Insights from Other Hydrogen-Metal Systems

Uranium hydride corrosion is an esoteric subject; in contrast, the corrosion of common structural metals such as zirconium, vanadium, titanium, and iron by environmental hydrogen has been of sustained and popular interest in the metallurgical community. While the broader topic of hydrogen-metal reactions goes beyond the scope of this report, some critical insights can be gained by examining a selected number of reports. A model for the hydrogen-induced embrittlement of Zr was developed and refined over a series of papers by Puls and co-workers; [58,59,60,61,62] the essential elements of this model also appear in more recent attempts to describe hydride precipitation and stress-induced growth, and subsequent crack propagation, in Zr and other hydride-forming metals (see, for example, the work of Varias and co-workers).[63] Significant parallel theoretical development and experimental work on these metals, contemporary to Puls and co-workers, was conducted by other researchers including Birnbaum and co-workers (see, for example, Refs. 64 and 65).

Three closely related, stress-based mechanisms have been identified which may affect the ability of hydrogen to dissolve into the metal lattice or, conversely, whether precipitation may be onset for given conditions of absorbed hydrogen concentration and temperature: 1) the terminal solid solubility (TSS) of hydrogen in the metal may be shifted to higher/lower temperatures with the application of tensile/compressive stress to the metal, due to differences in the partial molar

volume of hydrogen (i.e., the lattice expansion per mole of interstitially-dissolved hydrogen) in the hydride vs. the metal;[61] 2) the TSS may be shifted to higher/lower temperatures with the application of tensile/compressive stress to the metal, due to the elastic or plastic strain energy associated with lattice accommodation of the lower density precipitate;[62] 3) the hydrogen chemical potential in the metal is lowered/raised by the application of tensile/compressive stress to the metal, such that local hydride growth is aided/retarded.[64] The relative strength of these effects has been experimentally observed to vary amongst hydride-forming metals. For example, the first mechanism has been determined to be negligible for Nb and Zr due to nearly identical values of hydrogen partial molar volume in the hydride and metal.[62,66]

The shifting of the TSS has also been observed to occur depending on whether the phase transition (solvus) is traversed during heating (hydride dissolution) or cooling (hydride precipitation); this hysteretic effect, which depends primarily on the balance and interplay of the three mechanisms above, is observed for example on zirconium but not vanadium.[62] Puls notes that the solvus temperature increases for niobium and zirconium upon a cooldown transition, whereas a decrease would be expected because of compressive stress being exerted on the metal by the expanding hydride precipitate (Mechanism 2 above);[62] this anomalous behavior is speculated to be the result of additional interactions of the precipitate with nearby dislocation defects to offset the accommodation strain energy in the surrounding metal.

As detailed in Section 1.3.1, the close association of hydride precipitation (corrosion initiation) with defects has been documented in numerous microscopic studies of uranium. The theoretical results of Taylor and Lillard (LANL), presented in Section 1.4, predict that atomic hydrogen should favor dissolution in tensile strain fields, such as those that occur near or at defect structures in uranium.[51] A follow-up study by these authors also found that only in the vicinity of defects where the metal can readily expand – into boundaries, vacancies, and voids – can the local interstitially dissolved hydrogen concentration approach that required to form uranium hydride, whereas the global hydrogen solubility in the defect-free bulk lattice is negligible (Section 1.2).[56] Similar experimental observations and theoretical predictions have been reported for other hydride-forming metals. For example, iron in its ferritic α phase at room temperature (293 K) has a lattice solubility of approximately 30-40 atomic parts-per-billion of hydrogen;[67] the comparative value for uranium is 10.5 appm, which can be extrapolated from the higher temperature data of Powell (Section 1.2).[29] However, apparent solubilities in polycrystalline, cold-worked iron can be significantly higher (e.g., a few appm), where the additional hydrogen capacity is not at interstitial sites of the lattice, but at defects where hydrogen binding energies can be a larger by a factor of two or more (e.g., 0.62 eV).[67,68,69] The deviation between the ideal and measured solubilities for cold-worked metals vanishes at higher temperatures due to the annihilation of defects during thermal recovery; this explains why the room temperature solubility for uranium, extrapolated from temperatures above 667 K, should approach a representation of the implied defect-free lattice solubility. Flanagan and co-workers performed similar solubility measurements on palladium, and observed hydrogen solubility enhancements (e.g., 65% at 298 K) for cold-worked versus well-annealed specimens.[70,71] These authors also

examined palladium which was quenched from the melt, such that a large concentration of lattice vacancies, which normally annihilate at elevated temperatures, could be preserved upon cooling.[70] They found that such specimens exhibited no measureable increase in hydrogen solubility and, since similar vacancy concentrations were expected in the cold-worked metal, concluded that this type of defect was not responsible for the enhanced hydrogen capacity of the cold-worked metal. Dislocations, as mentioned at the conclusion of Section 1.4, are the hallmark of cold work; as such, they have been identified as the dominant defect type responsible for trapping hydrogen in metals processed by cold working.

Models for the interaction of atomic hydrogen with dislocations, primarily edge type, have been developed to explain measured solubility enhancements in cold-worked metals.[72] In particular, analytic formulas have been developed from continuum mechanics and thermodynamics, with the inclusion of stress effects on the hydrogen chemical potential in the metal (Mechanism 3 above);[71,72] these classical models cannot be applied directly at the dislocation itself, so atomistic approaches (e.g., those based on DFT) must be applied in this exclusion region dubbed the 'dislocation core.' Flanagan and co-workers showed that such models could predict the hydrogen solubility enhancement for cold-worked palladium over a range of temperatures (273-348 K) with an absolute error of less than ~11%, assuming a modeled dislocation core radius of three times the Burgers vector magnitude.[71] A more computationally intensive, atomistic approach on α-iron was reported by Psiachos, who also found a similar enhancement of H solubility in the tensile strain region immediately below the glide plane of an edge dislocation.[73] This DFT study reported enhancement of hydrogen binding energies in iron (equivalently, "solution energies") with tensile hydrostatic strain, approaching 0.56 eV at -0.02 in the dilute limit (i.e., dissolved H content approaching zero);[73] this calculated value compares favorably to those obtained experimentally by Kumnick and Johnson (0.62 eV)[69] and Riecke and Bohnenkamp (0.58 eV)[74] on cold-worked, high-purity iron. From internal friction measurements on cold-worked iron, lower H-dislocation energy values were inferred by Gibala (0.28 eV),[75] and Zielinski and co-workers (~0.3 eV).[76] As Wolfer and Baskes observed,[77] and Kumnick and Johnson acknowledged indirectly,[69] this discrepancy can be attributed to the presence of a range of binding energies within the stress field surrounding the dislocation, with the highest values at the core (in consistency with the DFT calculations of Psiachos) and the lowest values representing some average over the field. The calculation by Psiachos also notably included H-H interactions, which are expected to further increase the degree of H solubility enhancement at dislocations.[78,79] The region of lattice distortion, running longitudinally along and radially outwards (in a cylindrical sense) from the dislocation line, thus defines a localized region of enhanced hydrogen solubility which is sometimes referred to as a "Cottrell atmosphere" or "Cottrell cloud."[80] The radius of the distortion (or dilatation) field typically extends up to a nanometer or more, and the sequestered hydrogen concentration contained therein can greatly exceed the global solubility limits.[72] For example, Maxelon and co-workers prepared palladium sheets with highly localized H concentrations equivalent to 600 parts-per-thousand, whereas the bulk solubility limit at room temperature is only 10 parts-per-thousand.[81] These authors determined from small angle neutron

scattering data that the dislocation-trapped hydrogen contributed significantly to the total effective H solubility – for example, a ~28% contribution at a TEM-measured dislocation area density of 2.0×10^{15} m^{-2}; such a dislocation area density is representative of typical cold-worked metal specimens.[82]

Finally, H solubility enhancements at extended lattice defects have also been reported for several metals. Mütschele and Kirchheim reported a range of hydrogen binding energies (0.32±0.16 eV) at grain boundaries in palladium, derived indirectly from cathodic charging experiments.[83] In their comprehensive review, Myers and co-workers observed that the presence of non-metallic species at internal boundaries often augments H solubility.[72] As an example, Fukushima and Birnbaum directly confirmed the presence of deuterium at or near at least some grain boundaries in nickel using SIMS;[84] they estimated a large H binding energy of ~1.3 eV at those defects containing co-segregated sulfur, versus values considerably less than 1 eV in the absence of sulfur. Birnbaum and co-workers also used SIMS to confirm deuterium trapping at grain boundaries in nickel-vanadium alloys.[85] Hong and Lee reported a H binding energy of 0.11 eV at the interface between α-iron and cementite (Fe_3C), derived from permeation experiments using samples of varying phase interface area;[86] in contrast, Hirth reported a large H binding energy of 0.98 eV at the interface between TiC inclusions and iron.[68] As with dislocations, there have been theoretical investigations of hydrogen interactions with boundaries. In one recent example, the DFT calculations of Du and co-workers predict H trapping at certain grain boundaries in α- and γ-iron, with binding energies up to 0.18 eV.[87]

It should be apparent at this point that the behavior of hydrogen in uranium with respect to defects, as described in the experimental (Section 1.3.1) and theoretical (Section 1.4) literature, is highly similar to that observed in a variety of other metals. The literature review presented above underscores the close relationship that exists between: 1) the localized and spatially heterogeneous distribution of lattice defects facilely known to exist in any real metal specimen; 2) the localized stresses and resulting strain fields created by their presence, and; 3) the local solubility condition of dissolved hydrogen. In seeking to better understand the physical mechanisms which underlie uranium hydride corrosion initiation, it would be imprudent to attempt any sort of quantitative adaptation of the generic knowledge base on hydride-forming metals. However, the qualitative characteristics of hydrogen-defect interaction so strikingly shared by uranium, iron, and other metals suggest that at least some of the same root causative factors are at play in all of these cases. In the next and final section, a qualitative model for hydride corrosion initiation based on these likely factors – which constitute the 'consensus' view (Section 1.2) – is proposed for realistic uranium components; then, the report concludes with recommended treatments or reconditioning procedures which should help to forestall the onset of hydride corrosion.

1.6 Recommended Strategies for Mitigating Uranium Hydride Corrosion

1.6.1 Qualitative Model of Hydride Corrosion on Uranium Components

To conceive a strategy for mitigating or eliminating uranium hydride corrosion, one must first consider the starting condition of the uranium component which is to be treated. As described in Section 1.1, uranium will typically pick up hydrogen contamination early in its processing while it is hot and its solubility limit is elevated; for example, in a salt bath at 630°C and a hypothetical hydrogen fugacity of 1 atm,[88] uranium will have a solubility of 9.2×10^{19} atoms per cm^3 (1.9 atomic parts-per-thousand, or 8.1 wppm).[29] This interstitially dissolved hydrogen is homogeneously distributed throughout the metal during annealing, and precipitates upon cooling to room temperature. The apparent behavior of environmental hydrogen during subsequent corrosion on uranium (Section 1.3.1), predicted behavior of dissolved hydrogen in uranium (Section 1.4), and the apparent and predicted behavior of dissolved hydrogen in metals such as iron and palladium (Section 1.5), all indicate that the hydride precipitates will form at randomly occurring lattice defects throughout the bulk and at all external surfaces. Since these hydride precipitates were created at the beginning of the component life cycle, and will ordinarily persist through service life, these shall be referred to as 'pre-existing' to distinguish them from hydride which forms upon subsequent exposure to environmental hydrogen (i.e., corrosion). Such pre-existing hydride precipitates at the component surface will be protected by a thin layer of oxide which forms upon even brief exposures to air.

If the uranium is then subjected to subsequent machining, there may be surface chemical reactions between liquid media and the (metal)/(metal oxide)/(metal hydride) that yield gaseous hydrogen; these media include cutting fluids, coolants, lubricants, and degreasing agents. While common solvents like acetone are not expected to significantly react upon adsorption to uranium oxide at room tempearture,[89] water-based media must be carefully considered. During grinding and polishing, where the oxide is abraded away and the uranium exposed, the following ideal reactions are expected to occur:[90,91,92]

$$2H_2O(l) + U(s) \rightarrow UO_2(s) + 2H_2(g) \quad (2)$$

$$4H_2O(l) + 2UH_3(s) \rightarrow 2UO_2(s) + 7H_2(g) \quad (3)$$

Baker and co-workers (AWE) deduced from XRD data that the oxide product in Eq. 2 is slightly superstoichiometric ($UO_{2.06}$) and finely divided, while measurements of specific surface area yield a large value of 30 m^2/g;[90,91] assuming a uniform powder of spherical particulates with mass density 10.793 g/cm^3,[93] this area translates to a diameter of 20 nm (see Eq. 6). These authors also reported a small (2-9%) yield of UH_3 from the reaction of water with uranium.[90,91] Haschke (LANL) suggested that Eq. 3, to be consistent with the observations of Baker and co-workers,[90,91] and Newton and co-workers,[92] should actually yield an oxide hydride ($UO_{1.2}H_{0.6}$) product species.[94] No spatial selectivity is implied by Eq. 2 – water should react indiscriminately with the denuded uranium surface, where no accounting is made for the possibility of

energetically or structurally favored chemisorption sites on different grain facet orientations. However, the segregation of hydride precipitates to defects suggests that hydrogen gas evolved in their vicinity may locally attack uranium to form more hydride:

$$3H_2(g) + 2U(s) \rightarrow 2UH_3(s) \quad (4)$$

particularly if the oxide formed in Eq. 3 is also of a finely divided and porous nature. Since the mass densities of UO_2 (10.793 g/cm^3)[93] and UH_3 (10.92 g/cm^3)[95] are both lower than that of the parent metal (19.05 g/cm^3),[30] the reactions expressed in Eqs. 2 and 4 describe a considerable, relative expansion of the two product species. If these reactions occur in locations constrained by the metal, such as at an inclusion-metal interface, local plastic deformation and fracture may occur if the product species grow above a certain size threshold (e.g., a micron).[1] The uranium surface, after such a water-based abrasive treatment, is thus expected to have regions of porosity and void formation from metal expansion and H_2 gas evolution associated with defects; these mechanisms are shown schematically in Fig. 3. Recent SEM data by Siekhaus (LLNL) on uranium disks polished with a 1 μm aqueous diamond slurry seem to support this qualitative model (Fig. 3d, inset).[96] Inclusions themselves may also be affected by chemical interactions with water; for example, Scott and co-workers (AWE) used SEM to observe the formation of horn-like growths at the corners and edges of uranium monocarbide (UC) inclusions upon sustained exposure to water vapor.[97] In this study, X-ray diffraction analysis on TEM lamellae revealed these growths to be metaschoepite, a hydrated uranium(VI) oxide with the formula $UO_3 \cdot 1\text{-}2H_2O$; this identification was further supported by negative ion maps (H^-, O^-, OH^-) from complementary SIMS experiments, which were spatially matched to the growths apparent in secondary electron images. Cross sections obtained by focused ion beam (FIB) milling revealed the water-driven growth advancing into the inclusion volume, apparently consuming the carbide and yielding a porous product.[97] The following reaction was tentatively suggested to explain the data:

$$UC(s) + 4H_2O(g) \rightarrow UO_3 \cdot H_2O(s) + CH_4(g) + H_2(g) \quad (5)$$

Note that the generation of gases, combined with the brittle nature and low density (4.69-4.97 g/cm^3) of metaschoepite,[98] is consistent with the porosity and void formation apparent in the FIB cross sections. These authors also reported simultaneous oxide layer growth during the water exposure, which they attributed to the reaction listed above in Eq. 2. No evidence of such horn-like growth was observed in the LLNL SEM data; however, the time scale of the water-based abrasion (minutes) was shorter than most of the durations reported in the AWE study (hours to days). Given that Scott and co-workers observed wide temporal variations in hydrous growth initiation, while still considering differences between direct water immersion versus the AWE study condition of ~85% relative humidity, it is plausible that insufficient time had elapsed for appreciable consumption of carbide to have occurred in the LLNL experimental case, and/or that any brittle hydrated uranium oxide formed as loose spallation and was therefore washed away during the sample rinsing step following abrasion.

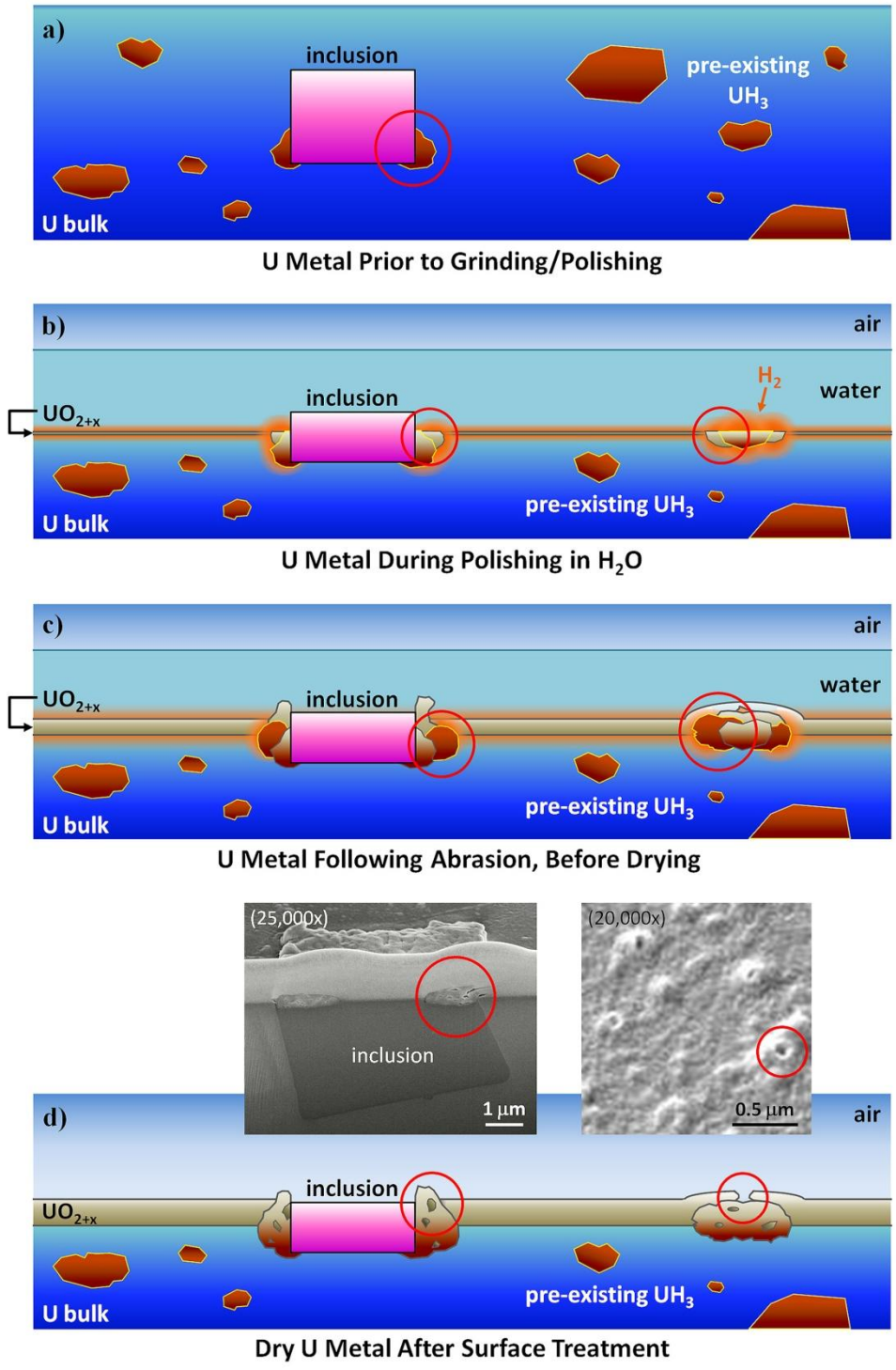

Figure 3. Surface reactions during water-based abrasion. a) Pre-existing UH_3 precipitates (open circle) at defects. b) Water reacts with exposed uranium and pre-existing UH_3, forming new oxide which is continuously abraded away and evolving H_2 gas (open circles). c) Abrasion ceases, wet sample develops persistent oxide layer; water continues to react with metal and UH_3; H_2 reacts with metal to form more UH_3 (open circles). d) Dry uranium surface with porous oxide growth at defect sites/pre-existing UH_3 precipitates; (inset) SEM images on water-polished uranium showing porous oxide features (Ref. 96).

After such possible preparations, the uranium component is presumed to enter service life; the surface of the metal, based on the discussion above, should have a microscopic morphology as shown in Figure 3d (schematic and inset). Even in the absence of water exposure, or other surface chemical reactions which may evolve gas and/or yield a lower density product, the uranium surface should have pre-existing hydride precipitates that are superficially oxidized upon handling in air.

Exposure to environmental hydrogen during this stage of the uranium component life cycle will eventually lead to hydride corrosion, with the most likely sites of initiation coinciding with the pre-existing surface precipitates and the defects at which they occur; recall from Section 1.4 the result of Balasubramanian (LLNL), whose quantum chemistry calculations indicated the catalytic behavior of uranium hydride towards the dissociation of molecular hydrogen.[55] The induction time which elapses between first hydrogen exposure and hydride initiation will depend on the factors discussed at the conclusion of Section 1.3.2, which all relate to the ability of atomic hydrogen to successfully penetrate through any oxide layer present to reach the uranium metal. As is apparent in Fig. 2e, nascent corrosion creates superficial micron-scale damage characterized by ductile fracturing, pulverization, and void formation; this pitting can be more easily seen in the corresponding FIB-milled cross section (Fig. 4). A comparison of the activation energies for uranium hydride formation on massive versus powdered samples reveals negative values in the latter case (Table 1). Such values, derived from Arrhenius plots of kinetics data, are unphysical and imply small or non-existent reaction barriers; as such, hydride corrosion should occur much more readily with powders than with massive samples. The uranium powder reaction data of Condon and Larson (Y-12) was accompanied by measurements of the specific surface area A_s using the Brunauer-Emmet-Teller method;[8] the powder values ranged from 0.3-2.3 m^2/g, which can be readily converted to nominal particle diameters assuming identical spheres of diameter d:

$$A_s = \frac{(sphere\ surface\ area)(number\ of\ spheres)}{1\ gram\ U} = \frac{(\pi d^2)N}{1\ gram\ U} = \pi d^2 \left[\frac{1}{(\rho_U)(\pi d^3/6)}\right]$$

$$d = \frac{6}{A_s \rho_U} \qquad (6)$$

where ρ_U is the mass density of α-uranium (19.05 g/cm^3).[30] The resulting size range d = 1.0-0.1 μm suggests that the micron-scale damage of corrosion, which bears a greater morphological

	Ref. 6	Ref. 9	Ref. 99	Ref. 11	Ref. 51[a]
Massive	10.5	26.6	18.8	28.5	0-27.2
Powder	-6.7	-6.7			
	Ref. 8	Ref. 99			

[a] Range of calculated values, corresponding to 1.4-0.5% tensile hydrostatic strain.

Table 1. Activation energies (kJ/mol) for uranium hydride formation on massive vs. powder samples.

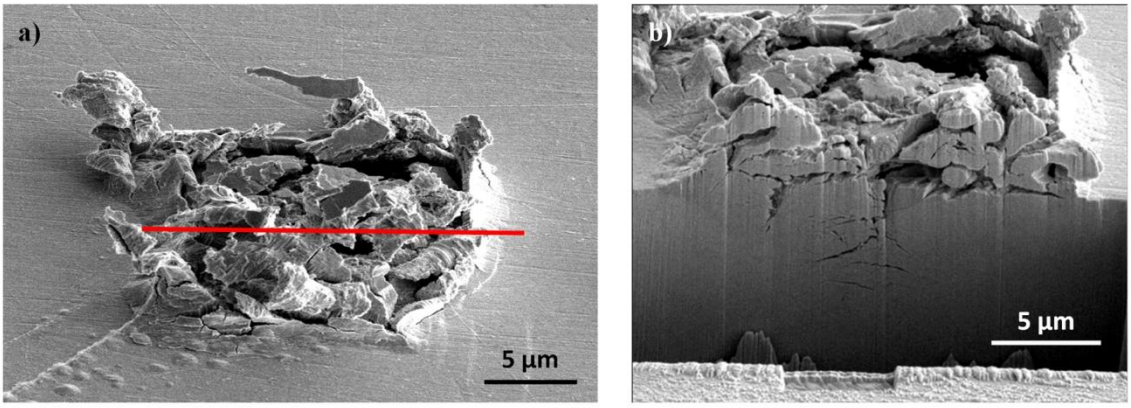

Figure 4. SEM images of a uranium hydride corrosion pit (from Ref. 18). a) External view, with position of cross section line indicated. b) FIB-milled cross section, showing internal damage.

similarity to powders than massive material, should have a high corrosion initiation potential compared to the surrounding intact metal.

One thus arrives at the expected condition of the uranium component at the outset of any corrosion prevention or remediation process. A newly manufactured part, if exposed to hydrogen contamination during its fabrication, will exhibit a spatially heterogeneous distribution of pre-existing hydride precipitates at defects; an enhanced oxide layer with localized porosity may also be present. A used part returned from service may also suffer from some corrosion damage, especially for aged items subjected to sustained exposure to environmental hydrogen. What can be done to the uranium component – whether new or used – to effectively minimize or eliminate its subsequent, deleterious interaction with environmental hydrogen?

1.6.2 Proposed Strategies

Any successful strategy for the mitigation or prevention of uranium hydride corrosion must not only obviously 'work', but be practically implementable and compatible with any requisite design parameters. Thus, regardless of the approach under consideration, certain guidelines must be acknowledged. Surface treatments are generally favored, since changes in bulk material properties (e.g., grain coarsening, precipitation hardening) may be undesirable or unacceptable. Design restrictions may preclude the application of potentially protective coatings. The cost of implementation and maintenance can be a more prohibitive factor than one of a technical nature. Therefore, methods which have the lowest projected non-recurring engineering costs and operational overhead – such as those which involve a simple modification of pre-existing equipment and facilities – are obviously ones which will have the greatest likelihood of adoption and integration into a manufacturing workstream.

Ion implantation has been previously reported as a mitigation strategy for uranium hydride corrosion. Various dopant species have been examined, including nitrogen (N_2^+),[100,101,102,103] carbon (C^+),[100,101,102,103,104] oxygen (O_2^+),[100,105] and sulfur (S^+).[100] A range of kinetic energies (80-

160 keV), and implantation doses (2×10^{16}-2×10^{18} ions/cm^2) and depths (up to ~400 nm), were studied; for example, an early study by Musket (LLNL) used 80 keV C^+ at 8×10^{17} cm^{-2}, resulting in a carbidic layer ~90 nm in depth.[104] In all cases, an increase in corrosion induction time was reported versus the unimplanted control samples; in the aforementioned LLNL study, the induction time was doubled under accelerated hydriding conditions (76 Torr H_2, 130°C), while Crusset and co-workers reported up to a 10x increase at lower hydrogen pressures (38 Torr H_2, 125°C).[100] Reductions in hydride area density and nucleation rate relative to the control samples were also reported by all researchers. A few mechanisms were proposed to explain the delay of corrosion onset and subsequent spatial and temporal reductions observed. Musket and co-workers (LLNL) suggested that dissolved oxygen anions, such as would occur in excess upon O_2^+ implantation, impeded the diffusion of hydrogen by competing for interstitial sites in the uranium lattice;[105] this competitive effect has been previously detailed in the uranium hydriding kinetics work of Condon and is generally accepted.[8,47] Ion-induced stress was commonly cited; Crusset and co-workers proposed that enhanced hydrogen binding should occur at locations affected by implantation,[100] in consistency with the body of literature reviewed in Sections 1.4 and 1.5. Arkush and co-workers (NRC-Negev), in the context of their hydride and oxidation corrosion mitigation studies using C^+ and N_2^+, proposed that the concentration gradient of dopant eased lattice mismatch stresses between the metal and overlying oxide by creating a less spatially abrupt transition;[102] the claimed result is the creation of an improved passivation layer towards environmental hydrogen resulting from greater adherence and mechanical integrity. To explain the incomplete protection afforded by this treatment against hydride corrosion, these authors suggested that certain defects such as carbide inclusions must persist after formation of the implant-fortified layer, providing locations of diffusive vulnerability to environmental hydrogen (Section 1.3.2).

There are some disadvantages to ion implantation treatment. Ion implantation is an intrinsically line-of-sight method with a limited ability to raster the beam across the target substrate; thus, while appropriate for electronic applications involving semiconductor wafers (as the most prominent example), it is poorly suited to three-dimensional components. Plasma immersion ion implantation is a different type of ion bombardment technique where the ionization is generated near the surface of the negatively-biased part, eliminating beam steering issues as well as permitting deeper and more rapid implantation;[106] however, the treated components are subjected to considerably elevated temperatures (e.g., 400°C). In any case, industrial grade ion implantation systems are expensive (multimillion dollar price point), and the radioactive nature of uranium would likely require the procurement of a dedicated instrument for component processing; therefore, a cost-benefit analysis for such a niche application may rule out this type of corrosion treatment.

Some insight can also be gained on the long-term stability of ion-implanted layers in uranium. Arkush and co-workers made XRD measurements on carbon- and nitrogen-implanted uranium at room temperature over the course of eight years, where the samples were stored in the

intervening periods in both ambient atmosphere and under 10^{-5} Torr vacuum conditions.[103] These authors observed changes which would negatively impact hydride corrosion resistance: 1) a severe reduction in crystallinity of the carbon-implanted surface layer (phase: UC_2) after three years in air, coupled with an inward diffusion of carbon; 2) a conversion of the UN_2 phase to the U_2N_3 phase after five years in air, with a concomitant loss of crystallinity and inward diffusion of nitrogen after three years. These changes were apparently less severe in the absence of air. In the case of the nitrogen-implanted layer, the phase transformation of UN_2 (face-centered cubic lattice with lattice parameter 5.31 Å)[107] to U_2N_3 (body-centered cubic lattice with lattice parameter 10.7 Å)[107] should increase the misfit stresses between the overlying oxide and underlying metal, in opposition to the claimed mechanism for increased corrosion protection. The very slow migration of carbon and nitrogen indicates exceedingly low diffusivities in uranium. Nitrogen implanted under similar conditions (40 keV, 7.5×10^{16} ions/cm^2) in 316 stainless steel has a diffusivity of 5.2×10^{-16} cm^2/s (673 K),[108] while hydrogen diffusivity in carbon steel is ~2×10^{-7} cm^2/s (293 K);[109] for comparison, the room temperature diffusivity of hydrogen in α-uranium is approximately 1×10^{-10} cm^2/s.[110] Therefore, carbon and nitrogen diffusivities in uranium are likely to be considerably less than 10^{-16} cm^2/s at room temperature; for example, if the implant diffusivity is 10^{-19} cm^2/s, the Fickian diffusion length after one year is $\sqrt{4Dt}$ = 35 nm, which is comparable to the layer depth of approximately 60 nm.[103] These estimates are therefore consistent with the temporal scale of thermal instability observed by Arkush and co-workers.

The series of papers by Arkush and co-workers explained the action of ion implantation in terms of its effects on the oxide layer, mitigating hydride corrosion by making it more difficult for environmental hydrogen to reach the uranium;[101,102,103] this is consistent with the NRC-Negev stance that the 'essential' causation for corrosion initiation lies with the oxide layer (and imperfections thereof) rather than the underlying metal (and imperfections thereof) (Section 1.3.2). However, in the spirit of the present report, strategies which focus on characteristics of the metal are now considered. In the previous section, several properties were identified as metal-borne drivers for subsequent hydride corrosion: 1) a spatially heterogeneous distribution of pre-existing hydride precipitates at defects; 2) an enhanced oxide layer with localized porosity and; 3) remnant corrosion damage. Sustained vacuum annealing at elevated temperatures (e.g., 500°C) is expected to purge the pre-existing hydride contamination from the surface and bulk by re-dissolution and outgassing.[88] A new or used uranium part subjected to this treatment will thus have an absence of these potent catalytic surface sites for atomic hydrogen production (Section 1.4), which should help retard the corrosion process. Nevertheless, both new and used components would still have misorientation boundaries, inclusions, possibly oxide porosity, and other defect types which are not eliminated by annealing; also, used components may have localized corrosion damage which possesses a powder-like, high corrosion potential (Section 1.6.1), and which also persist after heat treatments well below the melting temperature. The mechanisms which previously caused dissolved hydrogen contamination to precipitate at these

randomly occurring defects would again compel environmental hydrogen to initiate at the same locations in a pretreated or rehabilitated part (Section 1.6.1). Therefore, a thermal treatment alone would not be expected to provide protection from future hydride corrosion.

Any real component, fabricated using conventional metallurgical processes from polycrystalline massive metal, will always possess a defect-riddled morphology. The 'consensus' view, formed from the literature on uranium hydride corrosion, supports the correlation of hydride corrosion initiation to certain types of defects: misorientation boundaries and inclusions (Section 1.3.1). This correlation was argued to represent a truly causal relationship, citing a large body of circumstantial experimental and theoretical evidence for the uranium-hydrogen system and other hydride-forming metals (Sections 1.3.2 through Section 1.5). But if misorientation boundaries and inclusions have a high corrosion initiation potential, does this apply universally to all possible types of defects? Fortunately, the answer appears to be 'no,' and the computational study of Taylor and Lillard (LANL) provides some insight (Section 1.4). Their theoretical results predicted that atomic hydrogen is energetically disposed to dissolve into the uranium lattice in tensile strain fields, and hence, at or near defect structures;[51] however, they also found that hydride precipitation was most favorable at defects which could also locally accommodate interstitially dissolved hydrogen at concentrations approaching the requisite 3:1 H/U ratio.[56] This implies that defects may generally interact with and trap hydrogen, but that only some subset of them may also permit the aggregated hydrogen to precipitate out as the UH_3 corrosion product. Misorientation boundaries and inclusions evidently fall into the latter category. Dislocations are a prototypical representative of the former category; as discussed in Section 1.5, these defects generated by the cold working of metal have been identified as hydrogen trapping sites in a variety of metals, and the source of apparent enhancements in hydrogen solubility at low temperatures. Evidence of this behavior in uranium can be deduced from the SEM data of Siekhaus and co-workers (LLNL) shown in Fig. 4.[18] The corresponding uranium samples received a final polish using a 1 μm aqueous diamond slurry; the resulting superficial layer of plastic deformation – rich with dislocations, deformation twins, and voids – should have a depth which is comparable to the abrasive grit size .[111] In Fig. 4, the intact surface margins of the corrosion pit can be seen at several locations, and measure approximately 0.5 to 3 μm in thickness. Since the total air exposure was limited to several minutes, and given the relatively slow growth rates of oxide for uranium exposure to air and water,[20,97] the surface material displaced by the growing hydride should be mostly comprised of intact metal. Since the observed thickness of material coincides with the expected depth of cold work, it appears that the corrosion initiation potential of the dislocation-rich surface is reduced relative to the underlying metal. This would be expected if the dislocations trapped significant quantities of hydrogen in their dilatation fields (Section 1.5), effectively sequestering it, and preventing its diffusion to and aggregation at locations where hydride corrosion is energetically favorable.

It must be noted that cold working also generates a high density of twin boundaries; such defects have been directly observed to promote uranium hydride corrosion (Section 1.3.1), and should behave like grain boundaries rather than dislocations in facilitating the critical aggregation of

dissolved hydrogen necessary for precipitation to occur. Thomas and co-workers, in their study of shot-peened Ti alloy (IMI-834), attributed the proliferation of dislocation structures to relief of plastic strain in the vicinity of twin boundaries, which themselves represent a favored mode of strain accommodation at room temperature.[112] The SEM observations of Siekhaus and co-workers would seem to indicate that the copresence of corrosion-promoting twins with corrosion-retarding dislocations does not entirely cancel out the beneficial effects of the latter.

If these interpretations are correct, the inadvertent corrosion protection afforded by mechanical polishing can be deliberately enhanced by deepening the superficial cold work and thereby creating a thickened 'skin' on the uranium component that is resistant to corrosion by environmental hydrogen. Mechanical surface treatments, such as peening and burnishing, would not only create such a cold-worked 'skin' but also simultaneously efface surface defects and prior corrosion damage by plastic deformation. Shot peening (SP) is inexpensive to implement, but achieving a uniform surface treatment on three dimensional components can be difficult. Controlled plasticity burnishing (CPB), a technique developed by Lambda Technologies (Cincinnati, OH), can impart controllable amounts of both cold work and compressive residual stress to depths greater than a millimeter; the ball-based tooling is compatible with any computer numerical control (CNC) machine, and can therefore be applied to the workpiece with extreme precision in any modern machine shop.[113] In contrast to both SP and CPB, laser peening (LP) – a method developed by the Metal Improvement Co. (Paramus, NJ) in conjunction with LLNL – is designed to impart residual compressive stress with little cold work (1-2% vs. 10-50% for shot peening).[114] Since processes which create dislocations will also typically induce residual compressive stresses, it is instructive to consider the potential effects of such stresses. Compressive stress (and the associated strain) has the opposite effect of tensile stress (and associated strain) on hydrogen interstitial solubility (Section 1.4) – namely, compressive lattice strains should *increase* energetic barriers to dissolution. Researchers at NRC-Negev have cited the exertion of compressive stress upon hydride precipitates by both the surrounding metal bulk and overlying oxide (in the case of surface corrosion) as a mechanism for growth inhibition.[14,37] In his model for linear uranium hydride corrosion kinetics, Condon (Y-12) similarly presumed that each hydride precipitate would grow in size until the ultimate strength of the constraining metal was exceeded, leading to fracture and unhindered hydrogen flux.[9] One might expect that the presence of residual compressive stress would provide an additional measure of corrosion protection, but certainly only below the ultimate compressive strain of the uranium and likely with diminishing effectiveness once plastic deformation is onset; this translates to a hydride precipitate size threshold above which the parent metal can no longer retain the corrosion product in compression (likely on the order of a micron).[1]

The effect of peening on metal-hydrogen interactions have been examined in several studies. Ma and co-workers on $Ni_3(Si,Ti)$ alloy found that SP reduced the effect of environmental hydrogen embrittlement;[115] they attributed this beneficial effect to H trapping at dislocations or vacancies, but ruled out residual stress as a cause through careful pre- and re-deformation experiments. Wilde and Chattoraj observed that SP applied to chromoly steel reduced hydrogen permeation

and uptake by 50% at 100% peening coverage.[116] Contrary to the work of Ma and co-workers, these authors ruled out cold work as a cause after observing similar reductions in permeation flux between the peened and unpeened surfaces of their samples; they therefore concluded that the residual compressive stress found at both surfaces was the most likely source for decreased hydrogen uptake. Brass and co-workers obtained mixed results using SP on low-carbon and 304 stainless steels;[117] they reported apparent reductions in the steady-state hydrogen permeation flux of ~28% after SP, and ~54% after SP followed by a 320°C anneal in low-carbon steel. These authors attributed this beneficial effect to hydrogen trapping by cold-working defects, and speculated that the annealing enhancement was the result of increased trapping efficiency resulting from void coalescence and/or an aggregation of dislocations; the presence of these trapping sites in the cold-worked surface layer of both types of steel was confirmed with radiographic imaging using tritium as a contrast agent. On the other hand, SP on 304 stainless steel resulted in an increase of hydrogen embrittlement, due to the induction of a superficial martensitic phase transformation. Finally, San Marchi (Sandia National Laboratory), Zaleski (LLNL), and co-workers reported a null effect of LP on the nickel-base Alloy 22 with respect to H solubility.[118]

Despite the similarity in peening intensity and coverage, shot size, and even observed beneficial effects in the reduction of hydrogen permeation and absorption,[116,117] the reports of Wilde and Chattoraj, and Brass and co-workers, arrive at divergent conclusions on the underlying causes. One possible explanation may involve sample composition; the chromoly steel coupons used by Wilde and Chattoraj were rendered into the martensite phase, which Brass and co-workers identified as the reason why their 304 stainless steel samples, with surface enrichment in that phase, experienced enhanced hydrogen permeation relative to their low-carbon steel counterparts. Thus, the similarity of hydrogen uptake observed by Wilde and Chattoraj for both peened and unpeened surfaces may well have been due to the preponderant influence of the alloy phase. Despite this discrepancy, all of the other studies appear to support the notion of hydrogen trapping at defects and the suppression of hydride precipitation underlying the embrittlement/corrosion process. The null result of the LP study is also consistent, since this peening method imparts almost no cold work to the treated part; this indicates not only that dislocation generation is critical to increasing hydride corrosion resistance, but that the relative beneficial effect of residual compressive stress speculated upon above may not be significant after all.

Based on a careful consideration of the body of experimental and theoretical literature on uranium hydride corrosion, and other metal-hydrogen systems more generally, as well as a review of known studies on mechanical surface treatments of structural metals, controlled plasticity burnishing appears to be the most promising method for increasing the hydride corrosion resistance of uranium. The automated nature of CPB makes it amenable to production facilities, while the single-point contact of the tool allows very complex, three-dimensional surfaces to be treated, maximizing the flexibility of the technique. Compared to ion implantation, the initial investment costs are more modest; hardware procurement (control unit, hydraulic

system, custom CNC tools), delivery and installation, and operator training define an initial investment budget in the $500K range.[119]

The cold-worked layer produced by CPB is expected to have excellent long term stability under ambient conditions, as would be expected given the wide span of industrial applications for CPB, SP, and related techniques. Prevéy examined the thermal stability of SP on the nickel-base superalloy IN718 and found, for example, that annealing at 525°C induced a 20% decrease in cold work up to a depth of approximately 20 μm within a few hours;[120] however, non-zero cold work for depths 20-200 μm showed no significant changes after 100 hours at this temperature. This author also reported a considerable relaxation of residual compressive stress under the same conditions (e.g., ~30% reduction at 65 μm depth); as suggested by the null effect of LP on Alloy 22,[118] the beneficial effect of compressive stress on hydride corrosion resistance is probably insignificant compared to cold working. As another example, metallographic analysis of stainless steel steam turbine blades with 20 years of service showed intact microstructural deformation and depth with only minor abrasive wear on loaded mount surfaces.[121]

1.7 Conclusion

The corrosion of uranium by environmental hydrogen is a destructive process, where the formation of relatively low density hydride precipitates results in a progressive loss of mechanical and structural integrity. This superficial pulverization has been observed to follow a localized, spatially heterogeneous, and random pattern of initiation on uranium surfaces. A close examination of the literature on uranium hydride corrosion – including both experimental and theoretical studies – as well as the more extensive and rich body of work on other hydride-forming metals, leads to the observation of a number of common characteristics; these points of definitive agreement, culled from a diversity of sources and often approaching unaminity, effectively constitutes a ‘consensus’ view of the corrosion initiation phenomenon. These qualitative behaviors, most notably the close correlation of hydride corrosion initiation to metal defect sites, are strikingly shared by uranium, iron, and other metals, suggesting that at least some of the same root causative factors for corrosion operate in each of these cases. The enhancement of hydrogen dissolution within the strain fields of defects such as dislocations (‘trapping’), and the additional ability of some subset of these defects to promote local hydrogen aggregation into uranium hydride, are mechanisms which find wide support in the literature. Uranium components under consideration for corrosion mitigation treatment (either preventative or remediative) may have a number of conditions which make them vulnerable to subsequent corrosion damage: 1) a spatially heterogeneous distribution of pre-existing hydride precipitates at defects, which have a high corrosion initiation potential compared to the bulk metal; 2) an enhanced oxide layer with localized porosity, and; 3) remnant corrosion damage, which has a morphological similarity to powders versus massive metal, and are thus also expected to have a high corrosion initiation potential. Hydrogen can be effectively sequestered at dislocations, and thus hindered from diffusing to and aggregating at locations where hydride corrosion is

energetically favorable. Based on this notion, mechanical surface treatments are recommended which cause dislocations to proliferate and effectively create a thickened 'skin' on the uranium component that is resistant to corrosion by environmental hydrogen, while also simultaneously effacing surface defects and prior corrosion damage by plastic deformation.

This work was performed under the auspices of the U.S. Department of Energy by Lawrence Livermore National Laboratory under Contract DE-AC52-07NA27344.

---

[1] J.K. Lee, Y.Y. Earmme, H.I. Aaronson, K.C. Russell, "Plastic relaxation of the transformation strain-energy of a misfitting spherical precipitate – Ideal plastic behavior," Metallurgical Transactions A – Physical Metallurgy and Materials Science 11, 1837-1847 (1980).

[2] In contrast, the action of hydride precipitation *within* the metal bulk and the resulting effects on mechanical and structural integrity, constitutes *internal* hydrogen embrittlement (IHE). Studies on the IHE of uranium focus on changes in gross mechanical properties (e.g. through tensile testing) rather than characteristics of the surface corrosion process (e.g., kinetics) – see, for example: E. Garlea, J.S. Morrell, G.L. Powell, R.L. Bridges, "Effects of hydrogen on mechanical properties of cast uranium," Y-12 National Security Complex Technical Report Y/DZ-3075 (2010).

[3] H. Inouye, A.C. Schaffhauser, "Low-temperature ductility and hydrogen embrittlement of uranium – A literature review," Oak Ridge National Laboratory Technical Report ORNL-TM-2563 (1969).

[4] H.R. Gardner, J.W. Riches, Transactions of the American Society for Metals 52, 728-747 (1960).

[5] J.E. Burke, C.S. Smith, "The formation of uranium hydride," J. Am. Chem. Soc. 69 (1947) 2500-2502.

[6] W.M. Albrecht, M.W. Mallett, "Reaction of hydrogen with uranium," J. Electrochem. Soc. 103 (1956) 404-409.

[7] E. Wicke, Kl. Otto, "Über das system uran–wasserstoff und die kinetik der uranhydridbildung (The uranium-hydrogen system and the kinetics of uranium hydride formation)," Z. Phys. Chem. N.F. 31 (1962) 222-248.

[8] J.B. Condon, E.A. Larson, "Kinetics of the uranium-hydrogen system," J. Chem. Phys. 59 (1973) 855-865.

[9] J.B. Condon, "Calculated vs. experimental hydrogen reaction rates with uranium," J. Phys. Chem. 79 (1975) 392-397.

[10] J.B. Condon, "Nucleation and growth in the hydriding reaction of uranium," J. Less-Common Met. 73 (1980) 105-112.

[11] J. Bloch, M.H. Mintz, "Kinetics and mechanism of the U-H reaction," J. Less-Common Met. 81 (1981) 301-320.

[12] G.L. Powell, W.L. Harper, J.R. Kirkpatrick, "The kinetics of the hydriding of uranium metal," J. Less-Common Met. 172 (1991) 116-123.

[13] J.R. Kirkpatrick, J.B. Condon, "The linear solution for hydriding of uranium," J. Less-Common Met. 172-174 (1991) 124-135.

[14] J. Bloch, M.H. Mintz, "Types of hydride phase development in bulk uranium and holmium," J. Nucl. Mater. 110 (1982) 251-255.

[15] D. Moreno, R. Arkush, S. Zalkind, N. Shamir, "Physical discontinuities in the surface microstructure of uranium alloys as preferred sites for hydrogen attack," J. Nucl. Mater. 230 (1996) 181-186.

[16] M. Balooch, A.V. Hamza, "Hydrogen and water vapor adsorption on and reaction with uranium," J. Nucl. Mater. 230 (1996) 259-270.

[17] J.F. Bingert, R.J. Hanrahan, R.D. Field, P.L. Dickerson, "Microtextural investigation of hydrided α–uranium," J. Alloy Compd. 365 (2004) 138-148.

[18] G.L. Powell, R.K. Schulze, W.J. Siekhaus, "Corrosion of Uranium by Hydrogen at Low Hydrogen Pressures," in Effects of Hydrogen on Materials, edited by B. Somerday, P. Sofronis, R. Jones (ASM International, Materials Park, 2009) 556-561.

[19] G.C. Allen, J.C.H. Stevens, "The behavior of uranium metal in hydrogen atmospheres," J. Chem. Soc., Faraday Trans. 184 (1988) 165-174.

[20] G.L. Powell, A.G. Dobbins, S.S. Cristy, T.L. Clift, H.M. Meyers, J. Lucania, M. Milosevic, "The study of the oxidation of uranium by external and diffuse reflectance FTIR spectroscopy using remote-sensing and evacuable cell techniques," SPIE Proc. 2089 (1993) 214-215.

[21] A.J. Nelson, T.E. Felter, K.J. Wu, C. Evans, J.L. Ferreira, W.J. Siekhaus, W. McLean, "Uranium passivation by C^+ implantation: a photoemission and secondary ion mass spectrometry study," Surf. Sci. 600 (2006) 1319-1325.

[22] P. Morrall, D.W. Price, A.J. Nelson, W.J. Siekhaus, E. Nelson, K.J. Wu, M. Stratman, W. McLean, "ToF-SIMS characterization of uranium hydride," Philos. Mag. Lett. 87 (2007) 541-547.

[23] T.B. Scott, G.C. Allen, I. Findlay, J. Glascott, "UD_3 formation on uranium: Evidence for grain boundary precipitation," Philos. Mag. 87 (2007) 177-187.

[24] H.R. Gardner, J.W. Riches, "The effect of uranium hydride distribution and recrystallization on the tensile properties of uranium," USAEC R&D Report HW-43543 (1957).

[25] L.W. Owen, R.A. Scudamore, "A microscope study of the initiation of the hydrogen-uranium reaction," Corr. Sci. 6 (1966) 461-468.

[26] R.G. Musket, G. Robinson-Weis, R.G. Patterson, "Modification of the hydriding of uranium using ion implantation," Mat. Res. Soc. Proc. 27 (1984) 753-758.

[27] R. Arkush, A. Venkert, M. Aizenshtein, S. Zalkind, D. Moreno , M. Brill, M.H. Mintz, N. Shamir, "Site related nucleation and growth of hydrides on uranium surfaces," J. Alloys Compd. 244 (1996) 197-205.

[28] A. Loui, unpublished data (2011).

[29] G.L. Powell, "Hydrogen in uranium," Y-12 National Security Complex Technical Report Y/DZ-2797 (2007).

[30] CRC Handbook of Chemistry and Physics (90^{th} edition), edited by D.R. Lide (CRC Press, Boca Raton, 2009).

[31] R.P. Straetz, J.E. Draley, "A Study of the Reaction Rate Between Tuballoy Metal and Purified Hydrogen," U.S. Atomic Energy Commission Tech. Report CT-3044 (1945).

[32] P. Adamson, S. Orman, G. Picton, "The effects of hydrogen on the tensile properties of uranium when tested in different environments," J. Nucl. Mater. 33 (1969) 215-224.

[33] C.J. Beevers, G.T. Newman, "Hydrogen embrittlement in uranium," J. Nucl. Mater. 23 (1967) 10-18.

[34] R. Arkush, A. Venkert, M. Aizenshtein, S. Zalkind, D. Moreno, M. Brill, M.H. Mintz, N. Shamir, "Site related nucleation and growth of hydrides on uranium surfaces," J. Alloys Compd. 244 (1996) 197-205.

[35] S. Paek, D. Ahn, K. Kim, H. Chung, "Characteristics of reaction between hydrogen isotopes and depleted uranium," J. Ind. Eng. Chem. 8 (2002) 12-16.

[36] R.M. Harker, "The influence of oxide thickness on the early stages of the massive uranium-hydrogen reaction," J. Alloys Compd. 426 (2006) 106-117.

[37] Y. Ben-Eliyahu, M. Brill, M.H. Mintz, "Hydride nucleation and formation of hydride growth centers on oxidized metallic surfaces – Kinetic theory," J. Chem. Phys. 111 (1999) 6053-6060.

[38] J. Glascott, "Hydrogen and uranium," Sci. Technol. J. AWE 6 (2003) 16-27.

[39] S. Orman, G. Picton, J.C. Ruckman, "Uranium oxides formed in air and water in the temperature range 200-375°C," Oxid. Met. 1 (1969) 199-207.

[40] D.F. Sherman, D.R. Olander, "Hydrogen dissolution in and release from nonmetals – I. Uranium dioxide," J. Nucl. Mater. 166 (1989) 307-320.

[41] W.J. Siekhaus, unpublished data (2008).

[42] J. Glascott, P. Monks, unpublished data (2008).

[43] S.G. Bazley, J.R. Petherbridge, J. Glascott, "The influence of hydrogen pressure and reaction temperature on the initiation of uranium hydride sites," Solid State Ionics 211 (2012) 1-4.

[44] V.J. Wheeler, "Diffusion and solubility of hydrogen in uranium dioxide single crystals," J. Nucl. Mater. 40 (1971) 189-194.

[45] R.M. Harker, A.H. Chohollo, "Surface analytical study of uranium exposed to low pressures of hydrogen at ~80°C," Mat. Res. Soc. Proc. 1444 (2012) DOI:10.1557/opl.2012.1219.

[46] J.R. Petherbridge, personal communication (2010).

[47] J.B. Condon, "Alternative model for nonstoichiometry in uranium hydride," J. Phys. Chem. 79 (1975) 42-48.

[48] J. Bloch, D. Brami, A. Kremner, M.H. Mintz, "Effects of gas phase impurities on the topochemical-kinetic behavior of uranium hydride development," J. Less-Common Met. 139 (1988) 371-383.

[49] A. Danon, J.E. Koresh, M.H. Mintz, "Temperature programmed desorption characterization of oxidized uranium surfaces: Relation to some gas-uranium reactions," Langmuir 15 (1999) 5913-5920.

[50] D.F. Teter, R.J. Hanrahan, C.J. Wetteland, "Uranium hydride nucleation kinetics: Effects of oxide thickness and vacuum outgassing," Los Alamos National Laboratory Technical Report LA-13772-MS (2001).

[51] C.D. Taylor, R.S. Lillard, "Ab-initio calculations of the hydrogen-uranium system: Surface phenomena, absorption, transport, and trapping," Acta Materialia 57 (2009) 4707-4715.

[52] H.J. Svec, F.R. Duke, "Study of the kinetics of the reaction between uranium, H_2, HD and D_2," U.S. Atomic Energy Commission Tech. Report ISC-105 (1950).

[53] K. Balasubramanian, W. Siekhaus, B. Balazs, W. McLean, "Computational modeling of uranium corrosion and the role of impurities (Fe, Cr, Al, C, and Si)," Lawrence Livermore National Laboratory Conference Proceeding UCRL-CONF-216838 (2005).

[54] A.L. DeMint, J.H. Leckey, "Effect of silicon impurities and heat treatment on uranium hydriding rates," J. Nucl. Mater. 281 (2000) 208-212.

[55] K. Balasubramanian, W.J. Siekhaus, W. McLean, "Potential energy surfaces for the uranium hydriding reaction," J. Chem. Phys. 119 (2003) 5889-5900.

[56] C.D. Taylor, T. Lookman, R.S. Lillard, "Ab initio calculations of the uranium-hydrogen system: Thermodynamics, hydrogen saturation of α–U and phase-transformation to UH_3," Acta Materialia 58 (2010) 1045-1055.

[57] J. Bloch, M.H. Mintz, "The effect of thermal annealing on the hydriding kinetics of uranium," J. Less-Common Met. 166 (1990) 241-251.

[58] R. Dutton, M.P. Puls, in "Effects of Hydrogen on the Behaviour of Materials," edited by A.W. Thompson, I.M. Bernstein (American Institute of Mining, Metallurgical and Petroleum Engineers, New York, 1976) 516-524.

[59] R. Dutton, K. Nuttall, M.P. Puls, L.A. Simpson, "Mechanisms of hydrogen induced delayed cracking in hydride forming materials," Metall. Trans. A 8 (1977) 1553-1562.

[60] L.A. Simpson and M.P. Puls, "The effects of stress, temperature and hydrogen content on hydride-induced crack growth in Zr-2.5 Pct Nb," Metall. Trans. A 10 (1979) 1093-1105.

[61] M.P. Puls, "The effects of misfit and external stresses on terminal solid solubility in hydride-forming metals," Acta Metall. 29 (1981) 1961-1968.

[62] M.P. Puls, "Elastic and plastic accommodation effects on metal-hydride solubility," Acta Metall. 32 (1984) 1259-1269.

[63] A.G. Varias, A.R. Massih, "Hydride-induced embrittlement and fracture in metals – effect of stress and temperature distribution," J. Mech. Phys. Solids 50 (2002) 1469-1510.

[64] T.B. Flanagan, N.B. Mason, H.K. Birnbaum, "The effect of stress on hydride precipitation," Scripta Metall. 15 (1981) 109-112.

[65] D.S. Shih, I.M. Robertson, H.K. Birnbaum, "Hydrogen embrittlement of α titanium: *in situ* TEM studies", Acta Metall. 36 (1988) 111-124.

[66] R.L. Eadie, C.E. Coleman, "Effect of stress on hydride precipitation in zirconium-2.5% niobium and on delayed hydride cracking", Scripta Metall. 23 (1989) 1865-1870.

[67] K. Kiuchi, R.B. McLellan, "The solubility and diffusivity of hydrogen in well-annealed and deformed iron," Acta Metall. 31 (1983) 961-984.

[68] J.P. Hirth, "Effects of hydrogen on the properties of iron and steel," Metall. Trans. A 11A (1980) 861-890.

[69] A.J. Kumnick, H.H. Johnson, "Deep trapping states for hydrogen in deformed iron," Acta Metall. 28 (1980) 33-39.

[70] T.B. Flanagan, J.F. Lynch, J.D. Clewley, B. von Turkovich, "The effect of lattice defects on hydrogen solubility in palladium I. Experimentally observed solubility enhancements and thermodynamics of absorption," J. Less-Common Met. 49 (1976) 13-24.

[71] T.B. Flanagan, J.F. Lynch, "The effect of lattice defects on hydrogen solubility in palladium II. Interpretation of solubility enhancements," J. Less-Common Met. 49 (1976) 25-35.

[72] For details on models of hydrogen-dislocation interactions, see the excellent review (and references therein): S.M. Myers, M.I. Baskes, H.K. Birnbaum, J.W. Corbett, G.G. DeLeo, S.K. Estreicher, E.E. Haller, P. Jena, N.M. Johnson, R. Kirchheim, S.J. Pearton, M.J. Stavola, "Hydrogen interactions with defects in crystalline solids," Rev. Mod. Phys. 64 (1992) 559-617.

[73] D. Psiachos, "*Ab initio* parametrized model of strain-dependent solubility of H in α-iron", Modelling Simul. Mater. Sci. Eng. 20 (2012) 035011.

[74] E. Riecke, K. Bohnenkamp, "The influence of lattice imperfections in iron on hydrogen diffusion," Z. Metallkd. 75 (1984) 76-81.

[75] R. Gibala, "Internal friction in hydrogen-charged iron," Trans. Metall. Soc. AIME 239 (1967) 1574-1579.

[76] A. Zielinkski, E. Lunarska, M. Smialowski, "The interaction of hydrogen atoms and dislocations in irons of different purity," Acta Metall. 25 (1977) 551-556.

[77] W.G. Wolfer, M.I. Baskes, "Interstitial solute trapping by edge dislocations," Acta Metall. 33 (1985) 2005-2011.

[78] R. Kirchheim, "Interaction of hydrogen with dislocations in palladium – I. Activity and diffusivity and their phenomenological interpretation," Acta Metall. 29 (1981) 835-843.

[79] R. Kirchheim, "Interaction of hydrogen with dislocations in palladium – II. Interpretation of activity results by a Fermi-Dirac distribution," Acta Metall. 29 (1981) 845-853.

[80] A.H. Cottrell, B.A. Bilby, "Dislocation theory of yielding and strain ageing of iron," Proc. Phys. Soc. A 62 (1949) 49-62.

[81] M. Maxelon, A. Pundt, W. Pyckhout-Hintzen, R. Kirchheim, "Small angle neutron scattering of hydrogen segregation at dislocations in palladium," Scripta Mater. 44 (2001) 817-822.

[82] A.H.M. Krom, A.D. Bakker, "Hydrogen trapping models in steel," Metall. Mater. Trans. B 31B (2000) 1475-1482.

[83] T. Mütschele and R. Kirchheim, "Segregation and diffusion of hydrogen in grain boundaries of palladium," Scripta Metall. 21 (1987) 135-140.

[84] H. Fukushima, H.K. Birnbaum, "Surface and grain boundary segregation of deuterium in nickel," Acta Metall. 32 (1984) 851-859.

[85] H.K. Birnbaum, B. Ladna, E. Sirois, "Hydrogen segregation to grain boundaries and external surfaces," Z. Phys. Chem. N.F. 164 (1989) 1157-1164.

[86] G.W. Hong, J.Y. Lee, "The interaction of hydrogen and the cementite-ferrite interface in carbon steel," J. Mater. Sci. 18 (1983) 271-277.

[87] Y.A. Du, L. Ismer, J. Rogal, T. Hickel, J. Neugebauer, R. Drautz, "First-principles study on the interaction of H interstitials with grain boundaries in α- and γ-Fe", Phys. Rev. B 84 (2011) 144121.

[88] A. Sunwoo, D. Goto, "Effects of processing on microstructure and properties of α–uranium formed parts," Scripta Mater. 47 (2002) 261-266.

[89] R. King, H. Idriss, "Acetone reactions over the surfaces of polycrystalline UO_2: A kinetic and spectroscopic study," Langmuir 25 (2009) 4543-4555.

[90] M.M. Baker, L.N. Less, S. Orman, "Uranium compatibility studies part 6: The products and mechanism of the uranium-water and uranium hydride-water reactions," Atomic Weapons Research Establishment Technical Report AWRE-O-45/65 (1965).

[91] M.M. Baker, L.N. Less, S. Orman, "Uranium + water reaction. Part 1. – Kinetics, products and mechanism," Trans. Faraday Soc. 62 (1966) 2513-2524.

[92] A.S. Newton, J.C. Warf, F.H. Spedding, O. Johnson, I.B. Johns, R.W. Nottorf, J.A. Ayres, R.W. Fisher, A. Kant, "Uranium hydride. 2. Radiochemical and chemical properties," Nucleonics 4 (1949) 17-25.

[93] F. Grønvold, "High-temperature X-ray study of uranium oxides in the UO_2-U_3O_8 region," J. Inorg. Nucl. Chem. 1 (1955) 357-370.

[94] J.M. Haschke, "Reactions of plutonium and uranium with water: Kinetics and potential hazards," Los Alamos National Laboratory Technical Report LA-13069-MS (1995).

[95] J.J. Katz, E. Rabinowitch, "The Chemistry of Uranium: The Element, Its Binary and Related Compounds" (Dover, New York, 1961).

[96] W. Siekhaus, unpublished data (2012).

[97] T.B. Scott, J.R. Petherbridge, N.J. Harker, R.J. Ball, P.H. Heard, J. Glascott, G.C. Allen, "The oxidative corrosion of carbide inclusions at the surface of uranium metal during exposure to water vapour," J. Hazard. Mater. 195 (2011) 115-123.

[98] "Metaschoepite," in Handbook of Mineralogy, edited by John W. Anthony, Richard A. Bideaux, Kenneth W. Bladh, Monte C. Nichols (Mineralogical Society of America, Chantilly, 2003). http://www.handbookofmineralogy.org/.

[99] J.L. Stakebake, "Kinetics for the reaction of hydrogen with uranium powder," J. Electrochem. Soc. 126 (1979) 1596-1601.

[100] D. Crusset, F. Bernard, E. Sciora, N. Gérard, "Modification of the hydriding kinetics of U-0.2wt.%V alloy using ion implantations," J. Alloys Compd. 204 (1994) 71-77.

[101] R. Arkush, M. Brill, S. Zalkind, M.H. Mintz, N. Shamir, "The effect of N_2^+ and C^+ implantation on uranium hydride nucleation and growth kinetics," J. Alloys Compd. 330-332 (2002) 472-475.

[102] R. Arkush, S. Zalkind, M.H. Mintz, N. Shamir, "The role of the diffuse interface of implanted surface layers in preventing gas corrosion – Implantation of N_2^+ and C^+ in uranium," Colloids Surf. A 208 (2002) 167-176.

[103] R. Arkush, M.H. Mintz, G. Kimmel, N. Shamir, "Long-term amorphisation of C^+ and N_2^+ implanted layers on a uranium surface," J. Alloys. Compd. 340 (2002) 122-126.

[104] R.G. Musket, "Suppression of the uranium-hydrogen reaction using high-dose carbon implantation," Mat. Res. Soc. Proc. 93 (1987) 49-55.

[105] R.G. Musket, G. Robinson-Weis, R.G. Patterson, "Modification of the hydriding of uranium using ion implantation," Mat. Res. Soc. Proc. 27 (1984) 753-758.

[106] J.A. García, R.J. Rodríguez, "Ion implantation techniques for non-electronic applications," Vacuum 85 (2011) 1125-1129.

[107] R.E. Rundle, N.C. Baenziger, A.S. Wilson, R.A. McDonald, "The structures of the carbides, nitrides and oxides of uranium," J. Am. Chem. Soc. 70 (1948) 99-105.

[108] J. Hirvonen, A. Anttila, "Annealing behavior of implanted nitrogen in ALSI-316 stainless steel," Appl. Phys. Lett. 46 (1985) 835-836.

[109] E. Hörnlund, J.K.T. Fossen, S. Hauger, C. Haugen, T. Havn, T. Hemmingsen, "Hydrogen diffusivities and concentrations in 520M carbon steel under cathodic protection in 0.5M NaCl and the effect of added sulphite, dithionite, thiosulphate, and sulphide," Int. J. Electrochem. Sci. 2 (2007) 82-92.

[110] M.W. Mallett, M.J. Trzeciak, "Hydrogen-uranium relationships," Trans. ASM 50 (1958) 981-989.

[111] L.E. Samuels, G.R. Wallwork, "The nature of mechanically polished metal surfaces – The surface deformation produced during the abrasion and polishing of zinc," J. Inst. Metals 86 (1957) 43-48.

[112] M. Thomas, T. Lindley, D. Rugg, M. Jackson, "The effect of shot peening on the microstructure and properties of a near-alpha titanium alloy following high temperature exposure," Acta Mater. 60 (2012) 5040-5048.

[113] http://www.lambdatechs.com/controlled-plasticity-burnishing.html (accessed Oct. 9, 2012).

[114] R. Specht, F. Harris, L. Lane, D. Jones, L. Hackel, T. Zaleski, J. Halpin, M. Hill, W. Wübbenhorst, "Process control techniques for laser peening of metals", in *Shot Peening*, edited by L. Wagner (Wiley-VCH Verlag, Weinheim, 2006) 474-482.

[115] C.L. Ma, T. Takasugi, S. Hanada, "The effect of pre-deformation on environmental embrittlement of Ni_3(Si,Ti) alloys," Scripta Metall. 34 (1996) 1633-1639.

[116] B.E. Wilde, I. Chattoraj, "The effect of shot peening on hydrogen absorption by and hydrogen permeation through AISI 4130 steels," Scripta Metall. 26 (1992) 627-632.

[117] A.M. Brass, J. Chêne, G. Anteri, J. Ovejero-Garcia, L. Castex, "Role of shot-peening on hydrogen embrittlement of a low-carbon steel and a 304 stainless steel," J. Mater. Sci. 26 (1991) 4517-4526.

[118] C. San Marchi, T. Zaleski, S. Lee, N.Y.C. Yang, B. Stuart, "Effect of laser peening on the hydrogen compatibility of corrosion-resistant nickel alloy," Scripta Mater. 58 (2008) 782-785.

[119] N. Jayaraman (Lambda Technologies), personal communication (2011).

[120] P.S. Prevéy, "The effect of cold work on the thermal stability of residual compression in surface enhanced IN718," Proceedings of the 20th ASM Materials Solutions Conference (2000) 1-9.

[121] J. Jung, H. Lee, W. Lee, D. Kim, N. Jung, "Investigation of a shot-peened turbine blade after long-term use," Proceedings of the International Conference on Shot Peening (2008) 2008126.